H. MISCHAK ET AL. www.ejci-online.com

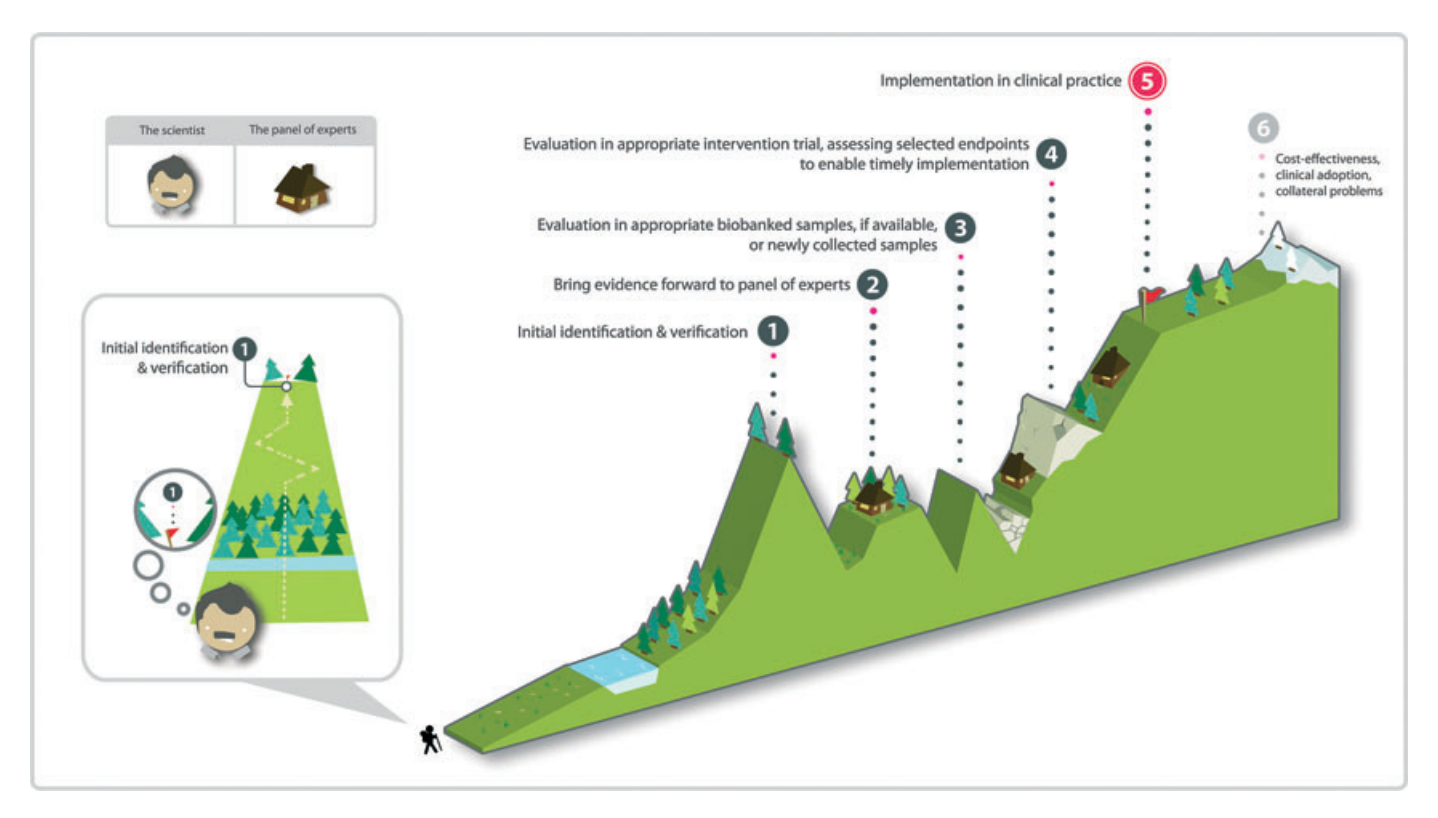


Figure 1 Implementation of novel biomarkers represents a substantially harder challenge than initially thought by scientists. As shown on the left-hand side of the cartoon, the current belief is that the major efforts are required during initial identification and verification of proteomics biomarkers. Implementation in the clinic is conceived as being simply a matter of continuing uphill, the 'last few steps' to the red flag. However, we argue that this is not true. While initial identification, verification and establishment of an appropriate analytical platform are without doubt major steps, even more substantial efforts are required on the road to actual implementation, which evidently is much longer than anticipated, and full of risks and additional obstacles. Among the major challenges are access to specific knowledge, sufficient funding, access to appropriate specimens, demonstration of reproducibility and performance of interventional trials. We propose support by a multidisciplinary panel immediately after initial verification, to accompany scientists on this road to implementation and to help avoid potentially useful biomarkers failing to reach the clinic. Once implementation in the clinic has been accomplished, the process does not stop, as cost-effectiveness, clinical adoption and collateral problems still must be monitored.

• Apply feedback mechanisms to evaluate cost-effectiveness, clinical adoption, problems in routine application, unanticipated collateral problems.

Key issues to settle in this process include the following:

• The definition of clinical needs and desired context of use for new biomarkers should be specifically emphasised [16]. Different approaches to establish research priorities may be considered: for example, expert committees, peer review, research-gap generation or value of information modelling. A key question is who should be involved in the process and how? Some countries have established organisations to

define and implement clinical priorities in a multidisciplinary and multistakeholder process, such as the Centre for Biomedical Network Research (CIBER) in Spain and the organisation INVOLVE of the UK Department of Health. Whether this is the optimal way to proceed remains to be seen. Generation of Web-based platforms allowing description of research priorities per disease and stakeholder (patient groups, health insurance companies, clinical societies, law-making bodies, etc.) appears to be a good starting-point to record existing views and to allow a more informed initiation of biomarker discovery efforts.

• A knowledgeable independent body or panel is required to evaluate the results of initial biomarker verification and qualification efforts as well as the respective claims and clinical utility in a transparent and unbiased manner. Currently, claims made for biomarkers are usually made by the scientists involved in the original studies, fostering unwarranted optimism and allegiance bias. The European Medicines Agency (EMA) and the US Food and Drug Administration (FDA) aim to provide evidence-based advice on biomarker qualification. One example is the voluntary biomarker qualification programme [33]. Biomarker data evaluation and guidance can be enhanced by the active involvement of a multidisciplinary panel (clinicians, clinical chemists, statisticians, health economists, representatives from patient groups, health insurance, pharmaceutical and biotechnology companies, (publicly funded) biobanks and regulatory agencies) that would evaluate existing data and provide specific recommendations for a road map towards clinical implementation of the biomarker for the specific context of use (including use of biobanked samples, surrogate and hard endpoints etc.; Fig. 1). Demonstration of reproducibility for markers that move towards clinical experimentation is vital; hence, evaluation should include repeatability checks by experienced statisticians/bioinformaticians using the raw data.

- Availability of funding for biomarker implementation studies. As an example, a certain part of the EU FP7 funding for collaborative projects under the Health theme is directed to clinical research projects, including investigator-driven clinical trials, to bring basic health research closer to the clinic (the 2011 call details can be found at http://ec.europa.eu/ research/participants/portal/page/cooperation?callIdentifier=FP7-HEALTH-2012-INNOVATION-1). Positive evaluation of biomarker data by the panel (II) could be regarded as a positive recommendation also for funding purposes. Such implementation-focused projects should involve representatives of all parties mentioned above, as partners or members of an advisory board, to ensure timely implementation.
- Increased accessibility to biobanks. Availability of appropriate and clinically well-documented samples is frequently a major bottleneck for biomarker studies, even if all other aforementioned gaps are filled. Biobanks can largely expedite the assessment of predictive or diagnostic ability of biomarkers. Use of samples from biobanks could rapidly provide answers regarding biomarker validity and guide (or spare) further qualification studies through prospective trials [34–38]. The EU-funded Biobanking and Biomolecular Resources Research Infrastructure (BBMRI) project (http:// www.bbmri.eu/) aims to build a coordinated, large-scale pan-European biobanking infrastructure, initially based on existing sample collections, resources, technologies and expertise [39]; it is intended to work as an interconnected node structure including biobanks, biomolecular resources, harmonised standards, databases and bioinformatics, as well

as a platform for assessing ethical, legal and societal issues. This approach is promising; however, it has not yet been fully realised, and substantial difficulties in accessing existing biobanks are encountered. In addition, harmonisation of quality control tools and sample collection protocols, both significantly influence the results obtained, has not been achieved yet, but is mandatory. These issues not only affect in vitro diagnostic tests [40] but also have a major impact on multiparametric '-omics' approaches and can override disease-related patterns or even abolish meaningful data interpretation.

Improvement efforts should be focused on transparency, creation of clear rules for sample accessibility and procedures for requests, including clear timelines; comprehensive listing of samples retrieved for all projects (outlining their type and the respective research project, so as to avoid duplication of efforts); streamlining of consent processes; and generation of the appropriate legislation that allows use of the stored samples. Stored samples should be associated with consent for the sample to be used in any scientific investigation. If analysing the sample is dependent on obtaining a new consent from the donor (who may well be deceased) individually for every experiment, then the value of such a biobank is minute, as its content can generally not be used because of this legal restriction.

Conclusion

Implementation of biomarkers is a complex process that would significantly benefit from the establishment of a general road map. While we have focused on proteomic biomarkers in this article, the considerations and suggestions extend well beyond the boundaries of the proteomics community and are relevant to all new biomarker technologies.

Potential consequences of implementation should be contemplated from the very beginning of the developmental process, even at the stage of biomarker discovery. We also suggest potential means to achieve these aims. Final success, the implementation of the biomarker to benefit patients, cannot be guaranteed upfront, even if the biomarker proves to be valuable, because there is a continuous evolution of the landscape, with all of its political, societal and clinical implications. The -omics revolution, and development of personalised medicine approaches, will add greater complexity and new challenges to the implementation process in the coming years. However, if mechanisms for efficient communication and guidance on a road map towards clinical implementation are apparent and disseminated, we will be much better equipped to react more promptly and make the required adjustments. The biomarker community will be better

H. MISCHAK *ET AL.* www.ejci-online.com

positioned overall to make more meaningful contributions to clinical care, which after all should be the principal goal of all parties involved.

Acknowledgements

This study is supported in part by the EuroKUP COST Action (BM0702) and the and by the European Community's 7th Framework Programme, grant agreement number HEALTH-F2-2009-241544 (SysKID). We would like to thank Aurelien Despierris for designing the cartoon (Fig. 1). Several of the authors are employed in part or fully by industry, and/or receive funding from industry, as also evident from their affiliations, but the article does not show partiality towards specific industry products or otherwise.

Disclaimer

TD: The views expressed are purely those of the author and may not in any circumstances be regarded as stating an official position of the European Commission. EM: The views expressed in this paper are the personal views of the author and may not be understood or quoted as being made on behalf of or reflecting the position of the European Medicines Agency or one of its committees or working parties.

Address

BHF Glasgow Cardiovascular Research Centre, Institute of Cardiovascular and Medical Sciences, College of Medical, Veterinary and Life Sciences, University of Glasgow, Glasgow G12 8TA, UK (H. Mischak, C. Delles, A. Dominiczak, N. Sattar); Mosaiques diagnostics, 30625 Hannover, Germany (H. Mischak); Clinical and Molecular Epidemiology Unit, Department of Hygiene and Epidemiology, University of Ioannina School of Medicine, 45110 Ioannina, Greece (J. P. A. Ioannidis); Stanford Prevention Research Center, Department of Medicine, Stanford University School of Medicine, Stanford, CA 94305, USA (J. P. A. Ioannidis); Department of Health Research and Policy, Stanford University School of Medicine, Stanford, CA 94305, USA (J. P. A. Ioannidis); Department of Statistics, Stanford University School of Humanities and Sciences, Stanford, CA 94305, USA (J. P. A. Ioannidis); RD Néphrologie, 34090 Montpellier Cedex, France (A. Argiles); Faculty of Life Sciences and School of Computer Science, University of Manchester, Manchester M13 9PL, UK (T. K. Attwood); Department of Immunology, Genetics and Pathology, Uppsala University, SE-751 24 Uppsala, Sweden (E. Bongcam-Rudloff); Department of Animal Breeding and Genetics, Swedish University of Agricultural Sciences, SE-751 24 Uppsala, Sweden (E. Bongcam-Rudloff); Sanofi-Aventis Deutschland GmbH D-65926 Frankfurt am Main, Germany (M. Broenstrup); Divisions of Histology and Biotechnology, Biomedical Research Foundation, Academy of Athens,

11527 Athens, Greece (A. Charonis); First Department of Pediatrics, Athens University Medical School, Aghia Sophia Children's Hospital, 11527 Athens, Greece (G. P Chrousos); European Commission, Directorate-General for Research and Innovation, Unit F5: Personalised Medicine, 21 rue du Champ de Mars, Brussels, Belgium (T. Dylag); Department of Pediatrics, Hannover Medical School, 30625 Hannover, Germany (J. Ehrich); IIS-Fundación Jiménez Díaz, Autonoma University, Madrid, Spain (J. Egido, A. Ortiz); C Institute of Clinical Chemistry, Universitätsklinikum Mannheim, 68167 Mannheim, Germany (P. Findeisen); Charité (CBF), Medizinische Klinik IV, 12200 Berlin, Germany (J. Jankowski); Abbott Laboratories, Abbott Park, IL 60064, USA (R. W. Johnson); Department of Medicine, University of Alabama at Birmingham, Birmingham, AL 35294, USA (B. A. Julien); Department of Gastroenterology, Hepatology and Endocrinology, Hannover Medical School, 30625 Hannover, Germany (T. Lankisch, M. P. Manns); The Beatson Institute for Cancer Research, Garscube Estate, Glasgow G61 1BD, UK (H. Y. Leung); Barbara Davis Center for Childhood Diabetes, University of Colorado Denver, Aurora, CO, USA (D. Maahs); Department of Experimental Medicine, University of Milano-Bicocca, Monza, Italy (F. Magni); European Medicines Agency, London, UK (E. Manolis); Medical University of Innsbruck, Department of Internal Medicine IV, 6020 Innsbruck, Austria (G. Mayer); Division of Nephrology, Department of Internal Medicine, University Medical Centre Groningen, University of Groningen, Groningen, The Netherlands (G. Navis); Department of Microbiology, University of Alabama at Birmingham, Birmingham, AL 35294, USA (J. Novak); Steno Diabetes Center, DK-2820 Gentofte, Denmark (F. Persson, P. Rossing); Baker Heart Research Institute, Melbourne, Vic. 8008, Australia (K. Peter); European Projects Office, Institute of Health Carlos III, Madrid, Spain (H. H. Riese); Department of Nephrology, Medical Faculty, University of Skopje, 1000 Skopje, Former Yugoslav Republic of Macedonia (G. Spasovski); Faculty of Medicine at Siriraj Hospital, Mahidol University, Bangkok 10700, Thailand (V. Thongboonkerd); Department of Nephrology, Ghent University Hospital, B 9000 Ghent, Belgium (R. Vanholder); Institut National de la Santé et de la Recherche Médicale (INSERM), U1048, Institut of Cardiovascular and Metabolic Disease and Université Toulouse III Paul-Sabatier, Toulouse, France (J. P. Schanstra); Division of Biotechnology, Biomedical Research Foundation, Academy of Athens, 11527 Athens, Greece (A. Vlahou).

Correspondence to: Harald Mischak, BHF Glasgow Cardiovascular Research Centre, Institute of Cardiovascular and Medical Sciences, College of Medical, Veterinary and Life Sciences, University of Glasgow, Glasgow, UK. Tel.: +44 141 330 6210; fax: +44 141 330 1689; e-mail: Harald.Mischak@glasgow.ac.uk

Received 17 March 2012; accepted 18 March 2012

References

- 1 Merchant ML, Perkins BA, Boratyn GM, Ficociello LH, Wilkey DW, Barati MT et al. Urinary peptidome may predict renal function decline in type 1 diabetes and microalbuminuria. J Am Soc Nephrol 2009;20:2065-74.
- 2 Good DM, Zürbig P, Argiles A, Bauer HW, Behrens G, Coon JJ et al. Naturally occurring human urinary peptides for use in diagnosis of chronic kidney disease. Mol Cell Proteomics 2010;9:2424-37.
- 3 Sethi S, Theis JD, Leung N, Dispenzieri A, Nasr SH, Fidler ME et al. Mass spectrometry-based proteomic diagnosis of renal immunoglobulin heavy chain amyloidosis. Clin J Am Soc Nephrol 2010;5:2180-7.
- 4 Spasovski G, Ortiz A, Vanholder R, El NM. Proteomics in chronic kidney disease: the issues clinical nephrologists need an answer for. Proteomics Clin Appl 2011;5:233-40.
- 5 Zurbig P, Dihazi H, Metzger J, Thongboonkerd V, Vlahou A. Urine proteomics in kidney and urogenital diseases: moving towards clinical applications. Proteomics Clin Appl 2011;5:256-68.
- 6 Anderson NL. The clinical plasma proteome: a survey of clinical assays for proteins in plasma and serum. Clin Chem 2010;56:177-85.
- 7 Semmes OJ, Feng Z, Adam BL, Banez LL, Bigbee WL, Campos D et al. Evaluation of serum protein profiling by surface-enhanced laser desorption/ionization time-of-flight mass spectrometry for the detection of prostate cancer: I. Assessment of platform reproducibility. Clin Chem 2005;51:102-12.
- 8 Haubitz M, Good DM, Woywodt A, Haller H, Rupprecht H, Theodorescu Det al. Identification and validation of urinary biomarkers for differential diagnosis and evaluation of therapeutic intervention in ANCA associated vasculitis. Mol Cell Proteomics 2009;8:2296-307.
- 9 Chau CH, Rixe O, McLeod H, Figg WD. Validation of analytic methods for biomarkers used in drug development. Clin Cancer Res 2008:14:5967-76.
- 10 Lee JW, Hall M. Method validation of protein biomarkers in support of drug development or clinical diagnosis/prognosis. J Chromatogr B Analyt Technol Biomed Life Sci 2009;877:1259-71.
- 11 Mischak H, Apweiler R, Banks RE, Conaway M, Coon JJ, Dominizak A et al. Clinical Proteomics: a need to define the field and to begin to set adequate standards. Proteomics Clin Appl 2007;1:148-56.
- 12 Ioannidis JP, Panagiotou OA. Comparison of effect sizes associated with biomarkers reported in highly cited individual articles and in subsequent meta-analyses. JAMA 2011;305:2200-10.
- 13 Biomarker bias. Nat Med 2012;17:763.
- 14 Diamandis EP. Cancer biomarkers: can we turn recent failures into success? J Natl Cancer Inst 2010;102:1462-7.
- 15 Knepper MA. Common sense approaches to urinary biomarker study design. J Am Soc Nephrol 2009;20:1175-8.
- 16 Mischak H, Allmaier G, Apweiler R, Attwood T, Baumann M, Benigni A et al. Recommendations for biomarker identification and qualification in clinical proteomics. Sci Transl Med 2010;2:46ps42.
- 17 Ioannidis JP. A roadmap for successful applications of clinical proteomics. Proteomics Clin Appl 2011;5:241-7.
- 18 Rifai N, Gillette MA, Carr SA. Protein biomarker discovery and validation: the long and uncertain path to clinical utility. Nat Biotechnol 2006;24:971-83.
- 19 Hood BL, Stewart NA, Conrads TP. Development of high-throughput mass spectrometry-based approaches for cancer biomarker discovery and implementation. Clin Lab Med 2009;29:115-38.
- 20 Boja ES, Jortani SA, Ritchie J, Hoofnagle AN, Tezak Z, Mansfield E et al. The journey to regulation of protein-based multiplex quantitative assays. Clin Chem 2011;57:560-7.

- 21 Remily-Wood ER, Liu RZ, Xiang Y, Chen Y, Thomas CE, Rajyaguru N et al. A database of reaction monitoring mass spectrometry assays for elucidating therapeutic response in cancer. Proteomics Clin Appl 2011;5:383-96.
- 22 Khleif SN, Doroshow JH, Hait WN. AACR-FDA-NCI Cancer Biomarkers Collaborative consensus report: advancing the use of biomarkers in cancer drug development. Clin Cancer Res 2010;16:
- 23 Sattar N. Biomarkers for diabetes prediction, pathogenesis or pharmacotherapy guidance? Past, present and future possibilities. Diabet Med 2012;29:5-13.
- 24 Ioannidis JP, Khoury MJ. Improving validation practices in "omics" research. Science 2011;334:1230-2.
- 25 Ioannidis JP, Tzoulaki I. What makes a good predictor?: the evidence applied to coronary artery calcium score. JAMA 2010;303:1646-7.
- 26 Fleming TR, DeMets DL. Surrogate end points in clinical trials: are we being misled? Ann Intern Med 1996;125:605-13.
- Ransohoff DF, Khoury MJ. Personal genomics: information can be harmful. Eur J Clin Invest 2010;40:64-8.
- 28 Ruggenenti P, Fassi A, Ilieva AP, Bruno S, Iliev IP, Brusegan V et al. Preventing microalbuminuria in type 2 diabetes. N Engl J Med 2004;351:1941-51.
- 29 Haller H, Ito S, Izzo JL Jr, Januszewicz A, Katayama S, Menne J et al. Olmesartan for the delay or prevention of microalbuminuria in type 2 diabetes. N Engl J Med 2011;364:907-17.
- 30 Dylag T, Jehenson P, van de Loo JW, Sanne JL. Basic and clinical proteomics from the EU Health Research perspective. Proteomics Clin Appl 2010;4:888-91.
- 31 Mischak H, Rossing P. Proteomic biomarkers in diabetic nephropathy-reality or future promise? Nephrol Dial Transplant 2010;25:2843-5.
- 32 Verma M, Wright GL Jr, Hanash SM, Gopal-Srivastava R, Srivastava S. Proteomic approaches within the NCI early detection research network for the discovery and identification of cancer biomarkers. Ann N Y Acad Sci 2001;945:103-15.
- 33 Manolis E, Vamvakas S, Isaac M. New pathway for qualification of novel methodologies in the European medicines agency. Proteomics Clin Appl 2011;5:248-55.
- 34 Keogh B. European biobanks forge cross-border ties. J Natl Cancer Inst 2011;103:1429-31.
- 35 Murtagh MJ, Demir I, Harris JR, Burton PR. Realizing the promise of population biobanks: a new model for translation. Hum Genet 2011;130:333-45.
- 36 Mitchell R, Conley JM, Davis AM, Cadigan RJ, Dobson AW, Gladden RQ. Genomics. Genomics, biobanks, and the trade-secret model. Science 2011;332:309-10.
- 37 Budimir D, Polasek O, Marusic A, Kolcic I, Zemunik T, Boraska V et al. Ethical aspects of human biobanks: a systematic review. Croat *Med J* 2011;**52**:262–79.
- 38 Kaye J. From single biobanks to international networks: developing e-governance. Hum Genet 2011;130:377-82.
- 39 Wichmann HE, Kuhn KA, Waldenberger M, Schmelcher D, Schuffenhauer S, Meitinger T et al. Comprehensive catalog of European biobanks. Nat Biotechnol 2011;29:795-7.
- 40 Poste G. Bring on the biomarkers. *Nature* 2011;469:156–7.
- 41 Chaturvedi N, Porta M, Klein R, Orchard T, Fuller J, Parving HH et al. Effect of candesartan on prevention (DIRECT-Prevent 1) and progression (DIRECT-Protect 1) of retinopathy in type 1 diabetes: randomised, placebo-controlled trials. Lancet 2008;372:1394–402.

H. MISCHAK ET AL. www.ejci-online.com

42 Sjolie AK, Klein R, Porta M, Orchard T, Fuller J, Parving HH et al. Effect of candesartan on progression and regression of retinopathy in type 2 diabetes (DIRECT-Protect 2): a randomised placebo-controlled trial. Lancet 2008;372:1385-93.

- 43 Bilous R, Chaturvedi N, Sjolie AK, Fuller J, Klein R, Orchard T et al. Effect of candesartan on microalbuminuria and albumin excretion rate in diabetes: three randomized trials. Ann Intern Med 2009;151:11-4.
- 44 Heart Outcomes Prevention Evaluation (HOPE) Study Investigators. Effects of ramipril on cardiovascular and
- microvascular outcomes in people with diabetes mellitus: results of the HOPE study and MICRO-HOPE substudy. Heart Outcomes Prevention Evaluation Study Investigators. Lancet 2000;355:253-9.
- 45 Patel A, MacMahon S, Chalmers J, Neal B, Woodward M, Billot L et al. Effects of a fixed combination of perindopril and indapamide on macrovascular and microvascular outcomes in patients with type 2 diabetes mellitus (the ADVANCE trial): a randomised controlled trial. Lancet 2007;370:829-40.

FISEVIER

Contents lists available at SciVerse ScienceDirect

European Journal of Pharmacology

journal homepage: www.elsevier.com/locate/ejphar



Pulmonary, gastrointestinal and urogenital pharmacology

Citrate, not phosphate, can dissolve calcium oxalate monohydrate crystals and detach these crystals from renal tubular cells

Somchai Chutipongtanate a,b,1, Sakdithep Chaiyarit a,b,1, Visith Thongboonkerd a,b,*

- a Medical Proteomics Unit, Office for Research and Development, Faculty of Medicine Siriraj Hospital, Mahidol University, Bangkok 10700, Thailand
- ^b Center for Research in Complex Systems Science, Mahidol University, Bangkok 10700, Thailand

ARTICLE INFO

Article history:
Received 25 January 2012
Received in revised form
31 May 2012
Accepted 9 June 2012
Available online 17 June 2012

Keywords:
Calcium oxalate
Citrate
Crystal
Dissolution
Kidney stone
Phosphate

ABSTRACT

Dissolution therapy of calcium oxalate monohydrate (COM) kidney stone disease has not yet been implemented due to a lack of well characterized COM dissolution agents. The present study therefore aimed to identify potential COM crystal dissolution compounds. COM crystals were treated with deionized water (negative control), 5 mM EDTA (positive control), 5 mM sodium citrate, or 5 mM sodium phosphate. COM crystal dissolution activities of these compounds were evaluated by phase-contrast and video-assisted microscopic examinations, semi-quantitative analysis of crystal size, number and total mass, and spectrophotometric oxalate-dissolution assay. In addition, effects of these compounds on detachment of COM crystals, which adhered tightly onto renal tubular cell surface, were also investigated. The results showed that citrate, not phosphate, had a significant dissolution effect on COM crystals as demonstrated by significant reduction of crystal size (approximately 37% decrease), crystal number (approximately 53% decrease) and total crystal mass (approximately 72% decrease) compared to blank and negative controls. Spectrophotometric oxalate-dissolution assay successfully confirmed the COM crystal dissolution property of citrate. Moreover, citrate could detach up to 85% of the adherent COM crystals from renal tubular cell surface. These data indicate that citrate is better than phosphate for dissolution and detachment of COM crystals.

© 2012 Elsevier B.V. All rights reserved.

1. Introduction

A major problem in management of COM kidney stone disease is its high recurrence rate as approximately 50% of the stone formers have recurrent stones within 10 years after the stone removal (Worcester and Coe, 2008). Although this recurrence rate tends to decline by prevention with high fluid intake (Borghi et al., 1996), dietary modifications (Borghi et al., 2002), and medical treatments (e.g., thiazide and alkali) (Pak, 2008), the recurrent stones remain in approximately 15–40% of cases who have received these interventions (Borghi et al., 2002; Coe et al., 2005; Fink et al., 2009), suggesting that the prevention against recurrent COM kidney stone disease require additional and better strategies.

Dissolution therapy has been widely accepted as an effective treatment for uric acid stone (Ngo and Assimos, 2007). It has been also investigated for many stone types, including calcium phosphate

(Xiang-bo et al., 2005), cystine (Tiselius, 2010), and struvite (Heimbach et al., 2000). Ideally, dissolution agents may be used as primary treatment to dissolve the whole calculi, adjuvant therapy to dissolve residual stone fragments after surgical removal, or prophylactic therapy to prevent recurrent stones (Ngo and Assimos, 2007). Unfortunately, this treatment modality has not been implemented for COM kidney stone disease due to the lack of strong evidence and characterizations of COM dissolution agents. EDTA, a well-known calcium-chelating agent, had been previously shown to have dissolution activity on COM stone in vitro (Burns and Cargill, 1987). However, the toxicity of this agent limits its applications in vivo (Kane et al., 1989; Oosterlinck et al., 1991). In contrast to uric acid stone, adjustment of urinary pH has minimal or no effect on the solubility of COM stone. Therefore, identification of COM stone dissolution agents, which are applicable in vivo, is needed for better management of COM kidney stone disease. Citrate and phosphate have been used for "prophylactic treatment" aiming to "prevent" recurrent COM kidney stone for a long time (Escribano et al., 2009; Tracy and Pearle, 2009). However, their "dissolution effects" on COM crystals, which are the major crystalline compositions of kidney stones, remained unclear and under-investigated.

The present study therefore aimed to evaluate COM crystal dissolution properties of citrate and phosphate using morphological evaluation and semi-quantitative measurement of COM

^{*}Corresponding author. at: Professor and Head of Medical Proteomics Unit, Director of Center for Research in Complex Systems Science (CRCSS), Siriraj Hospital, Mahidol University, 12th Floor Adulyadej Vikrom Building, 2 Prannok Road, Bangkoknoi, Bangkok 10700, Thailand. Tel./fax .: +66 2 4184793.

E-mail addresses: thongboonkerd@dr.com, vthongbo@yahoo.com (V. Thongboonkerd).

¹ Both authors share equal contributions.

crystal size, number and total mass. Serial analysis was performed by video-assisted morphological study to monitor the dissolution activities of these compounds within 1-h of the treatment. Validation of their dissolution activities was performed by spectrophotometric oxalate-dissolution assay to measure the increased levels of free oxalate ions as the end products of COM crystal dissolution. Finally, effects of these compounds on detachment of COM crystals, which were adhered tightly on renal tubular cell surface, were also investigated.

2. Materials and methods

2.1. COM crystal preparation and treatment with citrate and phosphate

COM crystals were generated according to our protocols published previously (Thongboonkerd et al., 2006; 2008). Briefly, COM crystals were prepared in 24-well, polystyrene, disposable cell culture cluster (with lid) (Corning Inc.; Corning, NY) by mixing calcium chloride (CaCl $_2 \cdot 2H_2O$) and sodium oxalate (Na $_2$ C $_2$ O $_4$) at final concentrations of 5.0 and 0.5 mM, respectively, in a buffer containing 10 mM Tris–HCl (pH 7.4) and 90 mM NaCl. After 1-h of COM crystallization, the supernatant was discarded, whereas the crystals were gently washed with 100% methanol and dried at room temperature (25 °C). These crystals were then used as a "blank" control.

To examine the dissolution effect, COM crystals were prepared as aforementioned, followed by an addition with 1-ml of dI water ("negative" control), 5 mM sodium EDTA (Na₄EDTA; final pH=9.49) ("positive" control), 5 mM sodium citrate (Na₃Citrate; Na₃C₆H₅O₇; final pH=8.48) (the normal range of urinary citrate is 1.5–7.5 mM (Chutipongtanate and Thongboonkerd, 2010)), or 5 mM sodium phosphate (NaH₂PO₄; final pH=5.70) (the normal range of urinary phosphate is 2.5–5.5 mM (Chutipongtanate and Thongboonkerd, 2010)). After 1-h incubation at room temperature (25 °C), dissolution effect of each treatment was evaluated as follows (all these experiments were done in triplicate).

2.2. Semi-quantitative analyses of COM crystal size, number and total mass

COM crystal dissolution effect of each treatment was initially screened by phase-contrast microscopic examination using an Olympus CKX41 inverted light microscope (Olympus Co. Ltd.; Tokyo, Japan). Crystal size was semi-quantitatively analyzed by ImageMaster 2D Platinum software (GE Healthcare; Uppsala, Sweden), which can accurately measure crystal area (Thongboonkerd et al., 2008). The crystal size was measured and averaged from at least 100 crystals in individual samples. Crystal number was counted and averaged from 10 high-power fields (HPF). Crystal mass, which is the most important parameter to evaluate dissolution activity, was then calculated by the following equation:

2.3. Video-assisted monitoring of COM crystal dissolution

Video-assisted dissolution study was performed to monitor the dissolution activity of each compound on COM crystals. COM crystal preparation and interventions were performed as described above but with video recording of dissolution events using a digital camera connected with Olympus CKX41 inverted phase-contrast microscope (Olympus Co. Ltd). The video files were replayed and images were

periodically extracted at various time-points, including 0, 1, 2, 5, 10, 30, and 60 min after the intervention. At each time-point, the crystal size was measured using ImageMaster 2D Platinum software (GE Healthcare) as aforementioned.

2.4. Spectrophotometric oxalate-dissolution assay

COM crystal dissolution would result to dissociation of CaOx molecules and increased levels of free calcium and oxalate ions in the solution. The increasing level of free oxalate ions was detectable by UV-visible spectrophotometry at $\lambda 214 \, \text{nm}$ (Nakagawa et al., 1985). Therefore, COM crystal dissolution activity could be measured using spectrophotometric oxalate-dissolution assay, which was modified from the oxalate-depletion assay used as the gold standard to quantitatively analyze COM crystal growth (Nakagawa et al., 1985). COM crystal seeds (160 µg) were added to a cuvette containing 1-ml of dI water in the absence or presence of 5 mM sodium EDTA, 5 mM sodium citrate, or 5 mM sodium phosphate. The mixture was continuously and gently stirred at room temperature (25 °C) using a mini-magnetic bar. Degree of oxalate resolution (which reflected degree of COM crystal dissolution) was then monitored for up to 60 min using a Shimadzu UV-160 A spectrophotometer (Shimadzu; Kyoto, Japan).

2.5. Investigation of COM crystal detachment

Detachment of COM crystals that tightly adhered on renal tubular cell surface was also investigated by video-assisted monitoring. Madin-Darby Canine Kidney (MDCK) cells (approximately 1×10^6 cells) were cultivated in complete Eagle's minimum essential medium (MEM) (GIBCO, Invitrogen Corporation; Grand Island, NY) supplemented with 10% fetal bovine serum, 1.2% penicillin G/streptomycin and 2 mM glutamine in 10-mm² dish inside a humidified incubator at 37 °C with 5% CO₂. The cells were maintained for approximately 24-h or until confluent monolayer was observed. Thereafter, the culture medium was removed and replace with the fresh medium containing COM crystals (100 µg COM crystals/ml MEM medium). The cells were further maintained for 1-h at 37 °C to allow COM crystals to adhere tightly onto MDCK renal tubular cell surface. Non-adherent crystals were then removed by three vigorous washes with PBS. To observe detachment of the adherent COM crystals, Na₄EDTA ("positive" control), Na₃Citrate or NaH₂PO₄ was added to 1-ml MEM medium to make the final concentration of 5 mM for each. An equal volume of dI water was also added to 1-ml MEM medium and used as the "negative" control. Final pH levels of MEM medium with Na₄EDTA, Na₃Citrate and NaH₂PO₄ were 7.69, 8.04 and 6.92, respectively. These media were added to the cells and the cells were further maintained for 1-h under video-assisted monitoring using a digital camera connected with Olympus CKX41 inverted phase-contrast microscope (Olympus Co. Ltd). The video images were periodically extracted at various time-points, including 0, 1, 2, 5, 10, 30, and 60 min after the intervention. At each time-point, the percentage of the remained adherent crystals was then calculated using the following equation:

% COM crystal detachment = $100x[(COMt_0 - COMt_n)/COMt_0]$ (2) where $COMt_0$ was the average number of the adherent crystals at basal time-point (0 min) and $COMt_n$ was the average number of the adherent crystals remained at any specific time-point. This experiment was also performed in triplicate.

2.6. Statistical analysis

All the quantitative data are reported as mean \pm S.E.M. Multiple comparisons were performed using ANOVA with Tukey's post-hoc

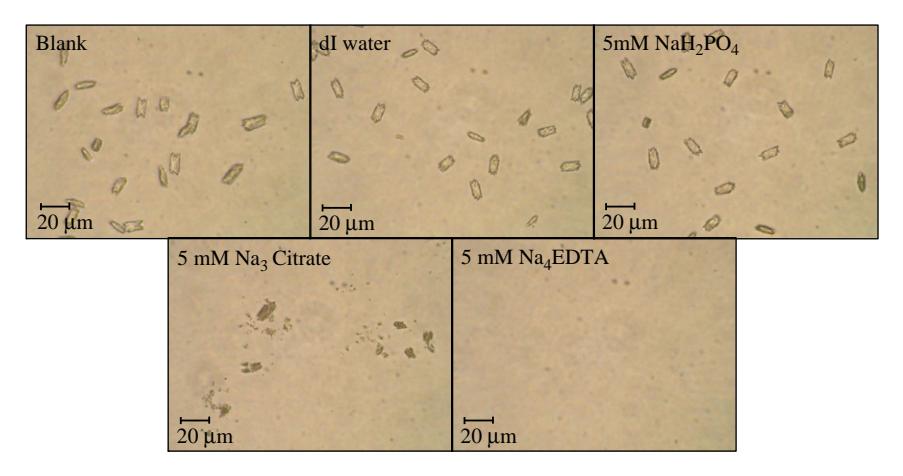


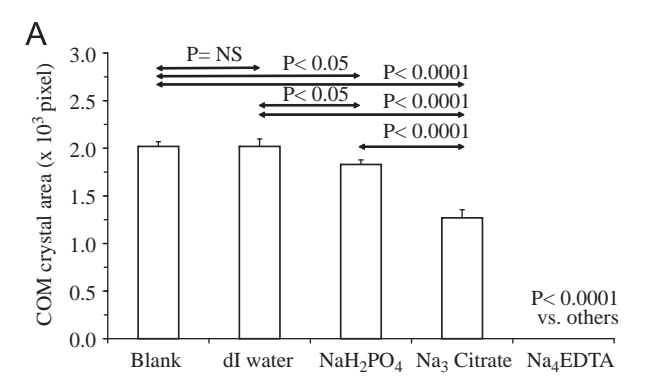
Fig. 1. Morphological evaluation of COM crystal dissolution effects. COM crystals were incubated for 1-h with dI water ("negative" control), 5 mM sodium EDTA (Na₄EDTA) ("positive" control), 5 mM sodium citrate (Na₃Citrate), or 5 mM sodium phosphate (NaH₂PO₄). COM crystals without any treatment served as the "blank" control. Images were taken from an Olympus CKX41 inverted light microscope (original magnification=400X for all panels). All experiments were done in triplicate.

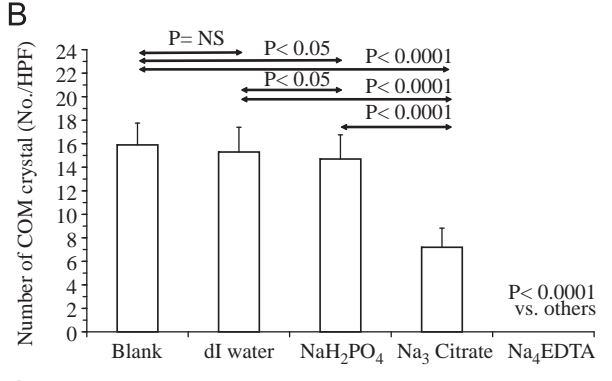
test (SPSS, version 11.5). P values < 0.05 were considered statistically significant.

3. Results

After 1-h incubation, COM crystal dissolution activities of 5 mM sodium citrate and 5 mM sodium phosphate were initially screened by phase-contrast microscopic examination using 5 mM sodium EDTA as the "positive" control and dI water as the "negative" control, whereas plain COM crystals without any addition served as the "blank" control. As expected, dI water had no effects on COM crystals, whereas sodium EDTA had a potent COM dissolution activity as demonstrated by complete dissolution of all COM crystals at 1-h post-incubation (Fig. 1). Treatment with sodium citrate also showed a significant dissolution effect on COM crystals but with a lesser potency as compared to sodium EDTA. In contrast, sodium phosphate had no obvious effects on COM crystals as the resulting crystals looked similar to those of blank and negative controls (Fig. 1).

At the same incubation time-point (1-h), crystal size, number and total mass were semi-quantitatively analyzed using Image-Master 2D Platinum software (GE Healthcare) to precisely evaluate the degree of dissolution effects of all compounds (Fig. 2). Consistent to the qualitative data as aforementioned, EDTA had a potent dissolution activity against COM crystals as all the crystals were completely dissolved after treatment with EDTA for 1-h. The dissolution effect of citrate was then compared to that of phosphate. For crystal size, phosphate slightly reduced COM crystal size (approximately 9% decrease), whereas citrate had much stronger effects (approximately 37% decrease) compared to negative and blank controls (Fig. 2A). This data suggested that semi-quantitative analysis using ImageMaster 2D Platinum software was more sensitive than qualitative analysis using phasecontrast microscopy to detect subtle changes in crystal size. For crystal number, only citrate was able to reduce COM crystal number (approximately 50% decrease) (Fig. 2B). This result implicated that some COM crystals (particularly the small ones) were completely dissolved within 1-h incubation with sodium citrate, whereas phosphate was not effective for COM crystal dissolution. Finally, the remaining COM crystal mass after dissolution was calculated (see Eq. (1) in the Materials and methods section). The data showed that citrate dramatically reduced COM total crystal mass (approximately 72% decrease), whereas phosphate reduced total crystal mass with a much lesser extent (approximately 16% decrease) (Fig. 2C). Taken together, these





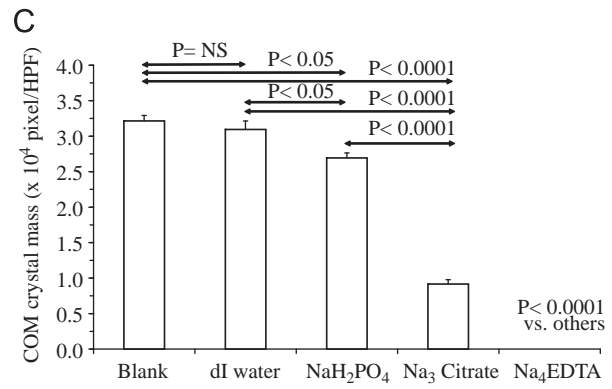
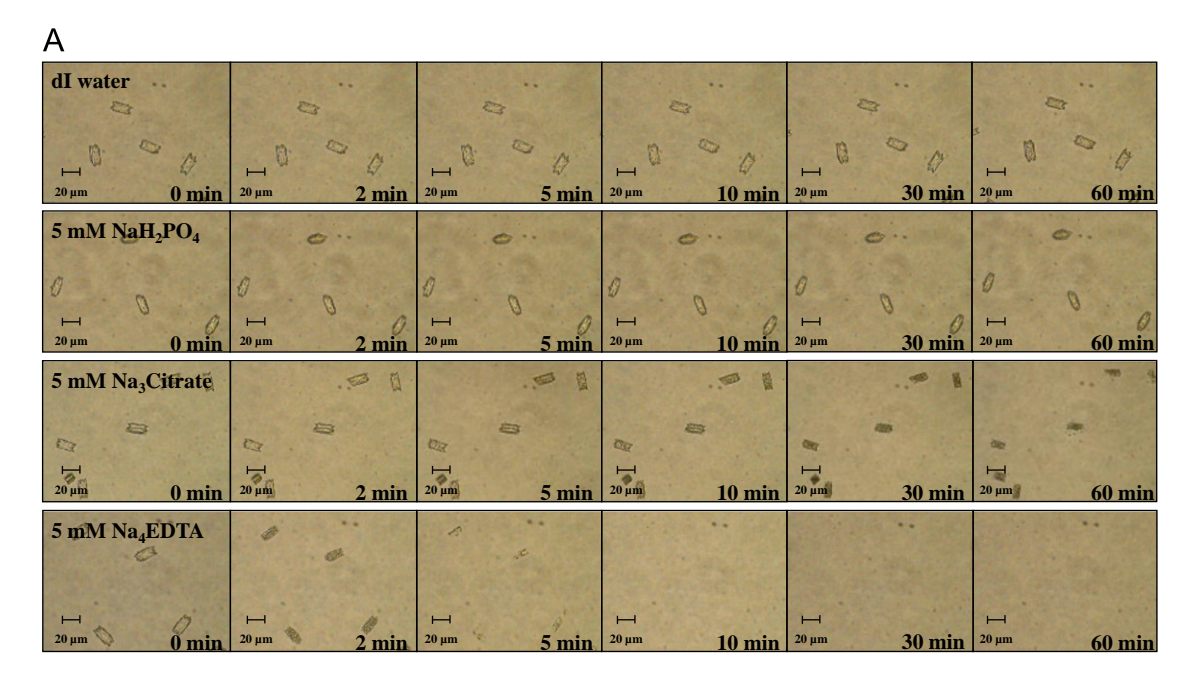


Fig. 2. Semi-quantitative analyses of COM crystal size (A), number (B) and total mass (C) after 1-h incubation of COM crystals with dI water ("negative" control), 5 mM sodium EDTA (Na₄EDTA) ("positive" control), 5 mM sodium citrate (Na₃Citrate), or 5 mM sodium phosphate (NaH₂PO₄). COM crystals without any treatment served as the "blank" control. Each bar was derived from 3 independent experiments and the data are reported as mean \pm S.E.M. NS=not significant.



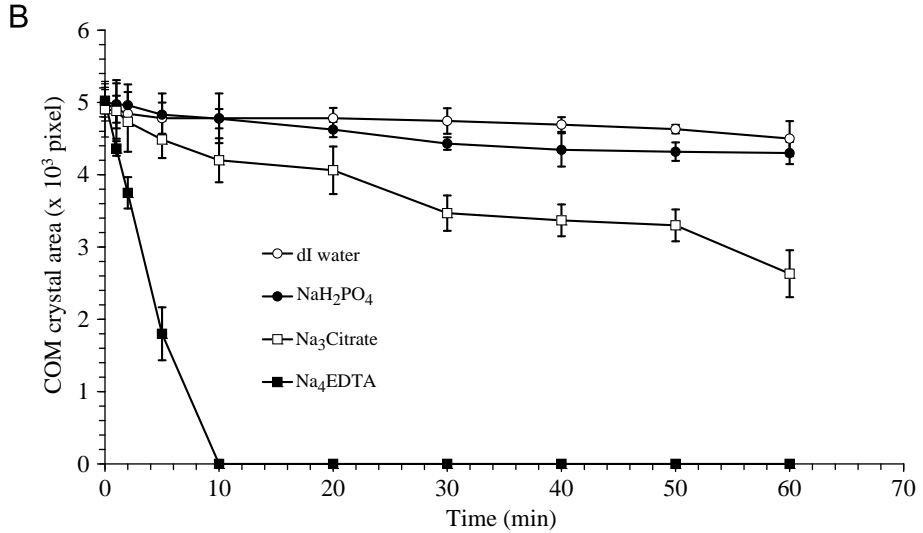


Fig. 3. Video-assisted COM crystal dissolution study. During 1-h incubation period of COM crystals with dI water, 5 mM sodium EDTA, 5 mM sodium citrate, or 5 mM sodium phosphate, the dissolution events were monitored and recorded using a digital camera (A). The video files were replayed and images were periodically extracted from various time-points. Thereafter, COM crystal size was serially measured at different time-points (B). The data are presented as mean ± S.E.M.

data indicated that citrate may be the better candidate to be used as a dissolution agent against COM crystals as compared to phosphate.

We initially examined effects of EDTA, citrate and phosphate at 1-h incubation period, at which the results were the final products of all spatial changes. We then monitored for serial changes of dissolution events within 1-h by video-assisted microscopic study (Fig. 3A). The results demonstrated that EDTA completely dissolved all COM crystals within 10-min, whereas citrate exhibited a gradual reduction of COM crystal size, starting from 20-min of incubation through the end of the assay (1-h). In contrast, phosphate did not show obvious dissolution activity (Fig. 3A and B).

The dissolution activities of these compounds were validated by spectrophotometric oxalate-dissolution assay (Fig. 4). Similar to the initial sets of data, EDTA had the strongest dissolution activity as demonstrated by a rapid increase in levels of free oxalate ions within only 10-min after incubation. Citrate also provided a potent dissolution activity, particularly at 1-h after incubation. It should be noted that, however, both dI water and sodium phosphate treatments were also associated with slightly increased levels of free oxalate ions. This phenomenon might be due to the physical interference in spectrophotometric oxalate-dissolution assay (in which the solution was continuously stirred), whereas this physical interference was absent in microscopic examinations (in which the solution was still, without stirring).

As pH of the solution might be the concern for evaluation of the dissolution activities of these compounds, we examined whether pH had an effect on COM crystal dissolution or not. As the final pH of the solution with 5 mM Na₄EDTA, 5 mM Na₃Citrate and 5 mM NaH₂PO₄ was 9.49, 8.48 and 5.70, respectively, we examined effects of pH 5.0–10.0 on COM crystal size and free oxalate levels using the assays described in the Materials and methods section (Video-assisted monitoring of COM crystal dissolution and Spectrophotometric oxalate-dissolution assay

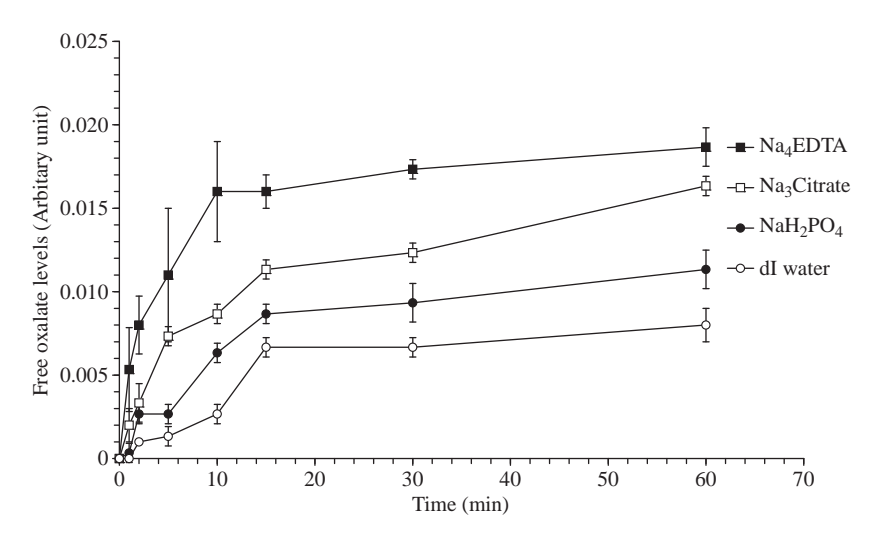


Fig. 4. Spectrophotometric oxalate-dissolution assay. COM crystal seeds ($160 \mu g$) were added to a cuvette containing 1-ml of dl water in the absence or presence of 5 mM sodium EDTA, 5 mM sodium citrate or 5 mM sodium phosphate. Levels of free oxalate ions (which reflected degree of COM crystal dissolution) was then serially monitored using absorbance at $\lambda 214 \mu m$ for up to 60 min. Each data point was derived from 3 independent experiments and the data are reported as mean \pm S.E.M.

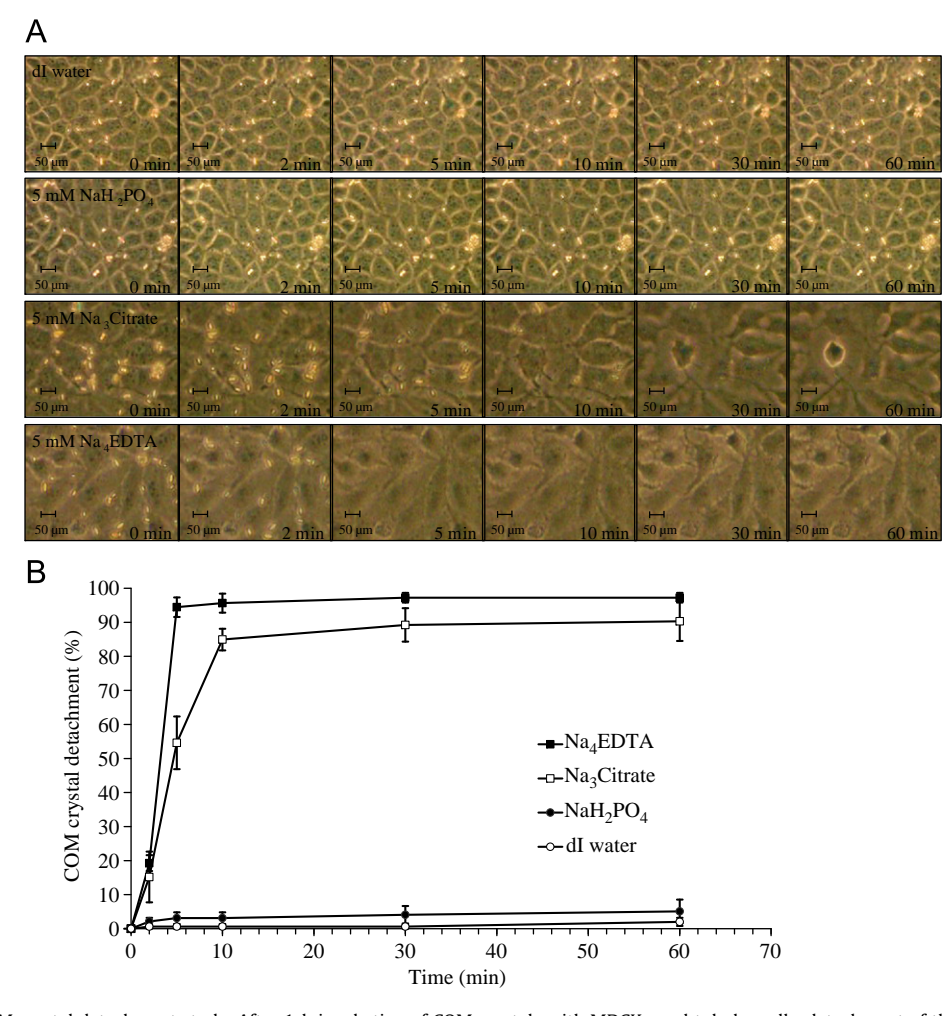


Fig. 5. Video-assisted COM crystal detachment study. After 1-h incubation of COM crystals with MDCK renal tubular cells, detachment of the adherent COM crystals by MEM medium containing dI water, 5 mM sodium EDTA, 5 mM sodium citrate, or 5 mM sodium phosphate were monitored and recorded using a digital camera (A). The video files were replayed and images were periodically extracted at various time-points. Thereafter, the number of remained adherent COM crystals was used for calculation of the degree of COM crystal detachment (B) (see Eq. (2) in the Materials and methods section). The data are presented as mean \pm S.E.M. (n=3 independent experiments for each data point).

sections), but without EDTA, citrate and phosphate. The pH of dI water was adjusted to 5.0–10.0 by concentrated HCl or NaOH. The data revealed that pH had no significant effects on COM crystal

dissolution (Supplementary Figs. S1 and S2). Thus, the effects of EDTA and citrate on COM crystal dissolution as aforementioned were not the results of their differential pH levels.

We extended our present study to also examine another mechanism of action of dissolution agent, i.e., crystal detachment activity (since dissociation of COM crystals at cell-crystal interface might disrupt adhesive force, particularly ionic interaction (Sheng et al., 2005), between the adherent COM crystals and apical surface of renal tubular epithelial cells. After allowing COM crystals to adhere tightly onto MDCK renal tubular cell surface for 1-h, the effects of all examined compounds on adherent COM crystals were monitored by video-assisted microscopic examination (Fig. 5A) and the degree of COM crystal detachment was calculated (see Eq. (2) in the Materials and methods section). Consistent with the other sets of data. EDTA rapidly dissolved and detached all COM crystals within 5-min. Citrate also showed the potent detachment activity (approximately 85% detachment) within 10-min after the treatment, whereas phosphate again showed no obvious detachment activities on the adherent COM crystals (Fig. 5A and Fig. 5B).

4. Discussion

Our present study successfully demonstrated COM crystal dissolution activity of citrate by direct measurements (i.e., morphological evaluation, semi-quantitative measurement of crystal size, number and total mass, as well as video-assisted study) and indirect measurement (i.e., spectrophotometric oxalate-dissolution assay). Note that we used sodium salts of all compounds (EDTA, citrate and phosphate) as to eliminate the effects of cations in our present study. Additionally, our preliminary data revealed that sodium chloride had no effects on COM dissolution (unpublished data). Therefore, any dissolution effects observed would be the results of EDTA, citrate or phosphate, not sodium.

Indeed, the dissolution effect of citrate against CaOx had been previously investigated by Saso et al. (1998) using an indirect assay of CaOx dissolution based on weight reduction of CaOx tablets (artificial packing of CaOx particulates). However, the analysis based only on weight reduction was considered as a rough approximation method. Another limitation was that CaOx tablet was artificial packing of CaOx particulates, which did not present crystalline faces and edges correlated with clinical calculi. In contrast, our present study performed a direct measurement of dissolution activity using a much higher sensitive method against clinically relevant COM crystals (both monoclinic prismatic and twin forms of COM prepared in this study are usually presented in the urine of stone formers (Thongboonkerd et al., 2006; 2008)). In addition, COM crystal detachment activity of citrate is reported herein for the first time. We hypothesized that citrate, as a small anionic molecule, may be able to penetrate into cell-crystal interface, and disrupt adhesive force between cells and crystals by calcium chelation and/or charge neutralization, resulting to COM crystal detachment. Better understanding of this mechanism of action may lead to rationally drug design and new strategy for medical management of COM kidney stone disease.

In contrast to citrate, phosphate seemed to have no significant benefit on COM crystal dissolution and detachment (yielded only minimal or modest degree of dissolution activity without a significant effect on crystal number and no detachment activity presented). Thus, phosphate is considerably ineffective to apply for COM stone dissolution therapy, whereas citrate provides much more potential advantages in management of COM kidney stone disease. Although it is unclear whether citrate administration is able to serve as primary therapy of COM stone or not, it should provide some benefits as an adjuvant therapy for elimination of residual stone fragments after surgical removal. This adjuvant therapy may facilitate dissolution and detachment of the retained COM crystals and/or fragments, especially those

adhered onto surface of urinary tract, thereby offers a better clearance of potential nuclei for recurrent stones. Moreover, dissolution and detachment activities of citrate provides a new insight into the prophylactic therapy of recurrent COM kidney stone disease as citrate not only prevents crystallization, growth and aggregation of COM crystals (Tracy and Pearle, 2009), but also dissolves the successfully formed COM crystals and detaches the adherent COM crystals from renal tubular cell surface.

5. Conclusions

In summary, our present study provided the direct evidence demonstrating that citrate at 5 mM concentration had COM crystal dissolution and detachment effects. Nevertheless, some concerns should be raised for citrate administration in routine clinical practice. It is still unknown what should be the appropriate dose that provides the optimal clinical outcome, which must balance between the dissolution efficacy and the adverse events, e.g., gastrointestinal complications (Fazil Marickar et al., 2010). This issue requires a prospective randomized clinical study to determine the optimal dose of citrate for dissolution and detachment therapy to reach the most favorable clinical outcome in COM kidney stone formers.

Acknowledgements

This study was supported by Office of the Higher Education Commission and Mahidol University under the National Research Universities Initiative, and The Thailand Research Fund (RTA5380005) to VT. VT is also supported by "Chalermphrakiat" Grant, Faculty of Medicine Siriraj Hospital.

Appendix A. Supporting information

Supplementary data associated with this article can be found in the online version at http://dx.doi.org/10.1016/j.ejphar.2012. 06.012

References

Borghi, L., Meschi, T., Amato, F., Briganti, A., Novarini, A., Giannini, A., 1996. Urinary volume, water and recurrences in idiopathic calcium nephrolithiasis: a 5-year randomized prospective study. J. Urol. 155, 839–843.

Borghi, L., Schianchi, T., Meschi, T., Guerra, A., Allegri, F., Maggiore, U., Novarini, A., 2002. Comparison of two diets for the prevention of recurrent stones in idiopathic hypercalciuria. N. Engl. J. Med. 346, 77–84.

Burns, J.R., Cargill III, J.G., 1987. Kinetics of dissolution of calcium oxalate calculi with calcium-chelating irrigating solutions. J. Urol. 137, 530–533.

Chutipongtanate, S., Thongboonkerd, V., 2010. Systematic comparisons of artificial urine formulas for in vitro cellular study. Anal. Biochem. 402, 110–112.

Coe, F.L., Evan, A., Worcester, E., 2005. Kidney stone disease. J Clin. Invest. 115, 2598–2608.

Escribano, J., Balaguer, A., Pagone, F., Feliu, A., Roque, I.F., 2009. Pharmacological interventions for preventing complications in idiopathic hypercalciuria. Cochrane Database Syst. Rev. CD004754.

Fazil Marickar, Y.M., Salim, A., Vijay, A., 2010. Effect of blind treatment on stone disease. Urol. Res. 38, 205–209.

Fink, H.A., Akornor, J.W., Garimella, P.S., MacDonald, R., Cutting, A., Rutks, I.R., Monga, M., Wilt, T.J., 2009. Diet, fluid, or supplements for secondary prevention of nephrolithiasis: a systematic review and meta-analysis of randomized trials. Eur. Urol. 56, 72–80.

Heimbach, D., Jacobs, D., Muller, S.C., Hesse, A., 2000. Improving cystine stone therapy: an in vitro study of dissolution. Urology 55, 17–21.

Kane, M.H., Rodman, J.S., Horten, B., Reckler, J., Marion, D., Vaughan Jr., E.D., 1989. Urothelial injury from ethylenediaminetetraacetic acid used as an irrigant in the urinary tract. J. Urol. 142, 1359–1360.

- Nakagawa, Y., Abram, V., Parks, J.H., Lau, H.S., Kawooya, J.K., Coe, F.L., 1985. Urine glycoprotein crystal growth inhibitors. Evidence for a molecular abnormality in calcium oxalate nephrolithiasis. J. Clin. Invest. 76, 1455–1462.
- Ngo, T.C., Assimos, D.G., 2007. Uric acid nephrolithiasis: recent progress and future directions. Rev. Urol 9, 17–27.
- Oosterlinck, W., Verbeeck, R., Cuvelier, C., Verplaetse, H., Verbaeys, A., 1991. Toxicity of litholytic ethylenediaminetetraacetic acid solutions to the urothelium of the rat and dog. Urol. Res. 19, 265–268.
- Pak, C.Y., 2008. Pharmacotherapy of kidney stones. Expert Opin. Pharmacother. 9, 1509–1518.
- Saso, L., Valentini, G., Leone, M.G., Grippa, E., Silvestrini, B., 1998. Development of an in vitro assay for the screening of substances capable of dissolving calcium oxalate crystals. Urol. Int. 61, 210–214.
- Sheng, X., Jung, T., Wesson, J.A., Ward, M.D., 2005. Adhesion at calcium oxalate crystal surfaces and the effect of urinary constituents. Proc. Nat. Acad. Sci. U.S.A. 102, 267–272.

- Thongboonkerd, V., Chutipongtanate, S., Semangoen, T., Malasit, P., 2008. Urinary trefoil factor 1 is a novel potent inhibitor of calcium oxalate crystal growth and aggregation. J. Urol. 179, 1615–1619.
- Thongboonkerd, V., Semangoen, T., Chutipongtanate, S., 2006. Factors determining types and morphologies of calcium oxalate crystals: Molar concentrations, buffering, pH, stirring and temperature. Clin. Chim. Acta 367, 120–131.
- Tiselius, H.G., 2010. New horizons in the management of patients with cystinuria. Curr. Opin. Urol. 20, 169–173.
- Tracy, C.R., Pearle, M.S., 2009. Update on the medical management of stone disease. Curr. Opin. Urol. 19, 200–204.
- Worcester, E.M., Coe, F.L., 2008. Nephrolithiasis. Prim. Care 35, 369-391.
- Xiang-bo, Z., Zhi-ping, W., Jian-min, D., Jian-zhong, L., Bao-liang, M., 2005. New chemolysis for urological calcium phosphate calculi—a study in vitro. BMC. Urol. 5. 9.



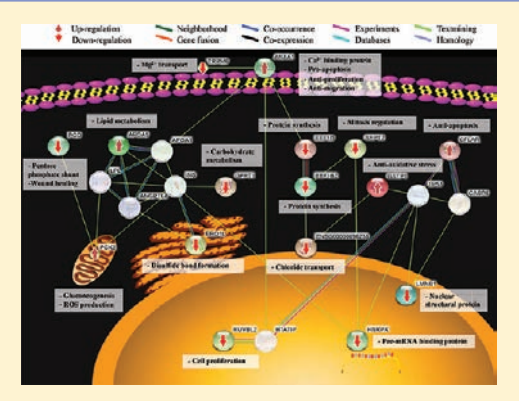
High Calcium Enhances Calcium Oxalate Crystal Binding Capacity of Renal Tubular Cells via Increased Surface Annexin A1 but Impairs Their Proliferation and Healing

Somchai Chutipongtanate, Kedsarin Fong-ngern, Paleerath Peerapen, and Visith Thongboonkerd*

[†]Medical Proteomics Unit, Office for Research and Development, Faculty of Medicine, Siriraj Hospital, and Center for Research in Complex Systems Science, Mahidol University, 10700 Bangkok, Thailand

Supporting Information

ABSTRACT: Hypercalciuria is associated with kidney stone formation and impaired renal function. However, responses of renal tubular cells upon exposure to high-calcium environment remain largely unknown. We thus performed a proteomic analysis of altered proteins in renal tubular cells induced by high-calcium and evaluated functional significance of these changes. MDCK cells were maintained with or without 20 mM CaCl₂ for 72 h. Cellular proteins were then analyzed by two-dimensional electrophoresis (2-DE) (n = 5gels derived from 5 independent culture flasks per group). Spot matching and quantitative intensity analysis revealed 20 protein spots (from a total of 700) that were differentially expressed between the two groups. These altered proteins were then identified by Q-TOF-MS and MS/MS analyses, including those involved in calcium binding, protein synthesis, carbohydrate metabolism, lipid metabolism, cell proliferation, mitosis regulation, apoptosis, cell migration, oxidative stress, and ion transport. Protein network analysis and functional



validation revealed that high-calcium-exposed cells had 36.5% increase in calcium oxalate monohydrate (COM) crystal-binding capacity. This functional change was consistent to the expression data in which annexin A1 (ANXA1), a membrane-associated calcium-binding protein, was markedly increased on the apical surface of high-calcium-exposed cells. Pretreatment with anti-ANXA1 antibody could neutralize this increasing crystal-binding capacity. Moreover, high-calcium exposure caused defects in cell proliferation and wound healing. These expression and functional data demonstrate the enhanced crystal-binding capacity but impaired cell proliferation and wound healing in renal tubular cells induced by high-calcium. Taken together, these phenomena may contribute, at least in part, to the pathogenic mechanisms of hypercalciuria-induced nephrolithiasis and impaired renal function. Our in vitro study offers several candidates for further targeted functional studies to confirm their relevance in hypercalciuria and kidney stone disease in vivo.

KEYWORDS: calcium, hypercalciuria, kidney, nephrolithiasis, proteomics, stone, tubular cells

INTRODUCTION

Hypercalciuria is defined as excessive urinary excretion of calcium (>200 mg/d in male; >150 mg/d in female) caused by several primary (or idiopathic) and secondary (i.e., genetic disorders, hormonal abnormalities, malignancies, and granulomatous diseases) etiologies.¹⁻⁴ Clinical significance of hypercalciuria is mostly resulted from its complications; i.e., impaired renal function and calcium oxalate monohydrate (COM) kidney stone disease (nephrolithiasis). 1,3,4 Vice versa, approximately 40% of COM stone formers have hypercalciuria. 4,5 It has been evidenced that high urinary calcium levels can enhance urinary COM supersaturation and thus facilitates COM crystallization, growth, and aggregation, leading to the development of COM nephrolithiasis. 4,6 Previous studies have demonstrated that highcalcium could enhance the adhesion of COM crystals onto renal tubular cell surface in a dose-dependent manner with still unknown mechanism(s). ^{7,8} The retained COM crystals can then grow further and/or aggregate with the nearby crystals, leading to

the formation of stone nidus and COM nephrolithiasis. This hypothesis has been supported by the correlation between urine calcium levels and clinical stone incidence.^{5,9} Despite some explanations for the lithogenic role of hypercalciuria (mostly chemical driven processes) in COM kidney stone formation, responses of renal tubular cells to this high-calcium environment (cellular driven processes) remain unclear. Whether these cellular driven processes play any significant roles, in return, to the development of COM nephrolithiasis remain unknown.

Another major complication of hypercalciuria is impaired renal function. Hypercalciuria due to some genetic disorders such as mutations of PCLN-1 gene 10 or CLCN5 gene 11 is associated with chronic kidney disease. Several lines of evidence have suggested that targeted intrarenal microstructure affected by hypercalciuria may be confined to renal tubules. $^{12-15}$ Electron microscopic

Received: January 23, 2012 Published: May 28, 2012

evaluation of the kidney derived from an animal model of hypercalciuria has shown dramatic histopathological changes in proximal and distal renal tubular cells, i.e., loss of brush border, apical vacuolization, and low-grade cell swelling. ¹⁵ In addition, clinical investigations in hypercalciuric patients have also demonstrated renal tubular dysfunctions. ^{12–14} Therefore, it is likely that defects in renal tubules may be the major mechanism for hypercalciuria-induced impaired renal function.

The present study aimed to evaluate cellular responses of renal tubular cells after exposure to high-calcium environment. Among several tubular cell types, distal renal tubular cell is most suitable for this study because, first, it plays a crucial role in renal calcium handling 16,17 and, second, it has been hypothesized to be a locale for COM crystals to interact with renal cells. 8,18 Madin-Darby Canine Kidney (MDCK) cells, which were derived from distal nephron and are used widely as the representing cells of distal renal tubules, ^{19,20} were examined for altered protein expression after exposure to the high-calcium environment by a gel-based proteomics approach, followed by protein network analysis. Thereafter, functional significance of the expression data predicted by protein network modeling was validated by highly focused functional studies, including enhanced COM crystalbinding capacity, impaired cell proliferation, and impaired wound healing.

MATERIALS AND METHODS

Cell Cultivation and Intervention

For proteomic analysis, MDCK cells were inoculated in 75 cm² culture flask (approximately 3×10^6 cells/flask; n=5 independent flasks per group). For functional studies of COM crystal-binding capacity, cell proliferation, cell death, and wound healing, MDCK cells were inoculated in a 6-well, polystyrene, cell culture cluster (with lid) (Corning Inc.; Corning, NY) (approximately 1×10^5 cells/well; n=3 wells per group in each experiment). For all experiments, the cells were maintained in complete Eagle's minimum essential medium (MEM) (GIBCO, Invitrogen Corporation; Green Island, NY) supplemented with 10% fetal bovine serum (FBS), 1.2% penicillinG/ streptomycin, and 2 mM glutamine, with or without the addition of 20 mM CaCl₂. Each culture medium was refreshed every day, and the cells were maintained in a humidified incubator at 37 °C with 5% CO₂ for 72 h before harvest.

For isolation of apical membranes, polarized MDCK cells were prepared by using Transwells (Costar; Cambridge, MA). Briefly, MDCK cells at a density of $5.0-7.5 \times 10^4$ cells/mL were plated and grown on a prewetted, collagen-coated, permeable polycarbonate membrane insert (0.4 μ m pore size) for 4 days. The culture medium (with or without the addition of 20 mM CaCl₂) was refreshed every other day. The collagen was coated onto the permeable polycarbonate membrane by dissolving collagen type IV powder (Sigma; St. Louis, MO) in 0.25% acetic acid at 4 °C. The collagen solution was then added onto the membrane insert (6–10 μ g/cm²) to cover the whole surface area of the membrane and incubated at 4 °C overnight before experiments.

Protein Extraction

After 72 h maintenance with or without 20 mM CaCl₂, the cell monolayer was harvested by directly scraping into the tube containing PBS. The cells were then washed with PBS three times. After the final wash, the cell suspensions were centrifuged at 10 000 rpm for 2-min, and the cell pellets were resuspended in a buffer containing 7 M urea, 2 M thiourea, 4% 3-[(3-min) area, 2 M thiourea, 4% 3-[(3-min) area, 2 M thiourea, 4% 3-[(3-min) area, 4

cholamidopropyl) dimethyl-ammonio]-1-propanesulfonate (CHAPS), 120 mM dithiothreitol (DTT), 2% ampholytes (pH 3-10), and 40 mM Tris-HCl, and further incubated at 4 $^{\circ}$ C for 30 min. Unsolubilized debris and particulate matters were removed by a centrifugation at 10 000 rpm for 2 min. Protein concentrations were determined using the Bradford method.

2-DE, Spot Matching, Quantitative Intensity Analysis, Q-TOF-MS, and MS/MS Analyses

For details of 2-DE, spot matching, quantitative intensity analysis, in-gel tryptic digestion, Q-TOF-MS, and MS/MS analyses, please see the Supporting Information.

Protein Network Analysis and Evaluation of Subcellular Localization

To obtain functional significance of the expression proteomics data, the Search Tool for the Retrieval of INteracting Genes/Proteins (STRING) software (http://string-db.org) was utilized.²¹ This publicly available software weighs and integrates the data on protein—protein associations, both physical (direct) and functional (indirect) interactions, from numerous sources including experimental repositories, computational predictions, and public literatures, which cover 2.5 million proteins from 630 organisms.²¹ By these extensive potential interactions, functional connectivity (or partnership) among the altered proteins derived from an expression proteomics study can then be assessed to generate a relevant protein association network.²¹ All the altered proteins in high-calcium-exposed MDCK cells were inputted into STRING 8.3 to retrieve the data for (i) protein function; (ii) subcellular localization; and (iii) protein interaction/functional connectivity.

2-D Western Blot Analysis to Confirm the Increased Level of ANXA1 in Whole Cell Lysate

Some of the proteomic data were confirmed by 2-D Western blot analysis, which has an advantage over the conventional 1-D Western blotting to observe expression levels and locales of multiple isoforms of a particular protein. Cellular proteins (an equal amount of 100 μ g total protein per sample) were resolved by 2-DE (as described above) and transferred onto nitrocellulose membranes (Whatman; Dassel, Germany) using a semidry transfer apparatus (Bio-Rad; Milano, Italy) at 75 mA for 1 h. Nonspecific bindings were blocked with 5% skim milk in PBS at room temperature for 1 h. The membranes were then incubated with mouse monoclonal anti-ANXA1 IgG1 (1:1000 in 5% skim milk/PBS) (Chemicon International, Inc.; Temecula, CA) at 4 °C overnight. After washing, the membranes were further incubated with rabbit antimouse IgG conjugated with horseradish peroxidase (1:2000 in 5% skim milk/PBS) (DakoCytomation; Glostrup, Denmark) at room temperature for 1 h. Immunoreactive protein spots were then visualized with SuperSignal West Pico chemiluminescence substrate (Pierce Biotechnology; Rockford, IL).

Isolation of Apical Membrane and Cytosolic Fractions and 1-D Western Blot Analysis to Confirm the Increased Surface Expression of ANXA1

Apical membranes of the polarized MDCK cells were isolated by a peeling method, of which principle is based on hydrous affinity and/or ionic interaction, as described previously. After culture with or without CaCl₂ for 72 h, the culture medium was removed, and the polarized cells were rinsed twice with ice-cold membrane preserving buffer (1 mM MgCl₂ and 0.1 mM CaCl₂ in PBS). Thereafter, Whatman filter paper (0.18 mm thick, Whatman International Ltd.; Maidstone, UK) prewetted with deionized

water was placed onto the polarized cell monolayer. After 5 min of incubation, the filter paper was peeled out, and the apical membranes retained at the paper surface were harvested by rehydration in deionized water and gentle scrapping. This apical membrane-enriched fraction was then lyophilized and subjected to protein extraction. The remaining cells were also harvested by scrapping and centrifuged at 10 000g for 10 min. The pellet was discarded, and the supernatant was collected as a cytosolic fraction. 1-D Western blot analysis was performed to evaluate the apical surface and cytosolic expression of ANXA1. All the procedures for 1-D Western blot analysis were similar to those for 2-D Western blot analysis, except only SDS-PAGE that was used to separate proteins (20 μ g total protein per lane) instead of 2-DE.

Laser-Scanning Confocal Microscopic Examination to Confirm the Increased Surface Expression of ANXA1

Apical surface expression of annexin A1 was also examined by laser-scanning confocal microscopy. Briefly, MDCK cells (approximately 1×10^5 cells per sample) were cultivated on coverslips (cleaved mica disk diameter: 9.5 mm, V-1 grade, SPI supplier; Toronto, Canada). After the cells were maintained with or without 20 mM CaCl2 for 72 h, they were rinsed with membrane preserving buffer (1 mM MgCl₂ and 0.1 mM CaCl₂ in PBS) and fixed with 3.7% formaldehyde in PBS at 25 °C for 15 min. After extensive washing with membrane preserving buffer, the cells were incubated with mouse monoclonal anti-ANXA1 (1:50 in 1% BSA/PBS) at 37 °C for 1 h. The cells were then rinsed with PBS three times and then incubated with AlexaFluor-488-conjugated goat antimouse IgG (Invitrogen/Molecular Probe; Burlington, Canada) (1:5000 in 1% BSA/PBS) containing 0.1 μ g/mL Hoechst dye (DNA staining for nuclear localization) (Invitrogen/Molecular Probes) at 37 °C for 1 h. Thereafter, the coverslips were mounted with 50% glycerol/PBS for subsequent examination of the XY, XZ, and YZ planes using a laser-scanning confocal microscope equipped with an LSM5 Image Browser (LSM 510 Meta, Carl Zeiss; Jena, Germany).

COM Crystal-Binding Assay

COM crystals were generated according to our protocols published previously. 23 MDCK cells were cultivated in a 6-well, polystyrene, disposable cell culture cluster (with lid) with or without 20 mM CaCl₂ for 72 h as described above. Thereafter, the culture medium was removed, and the cells were washed with warm PBS twice and incubated with 1% BSA in membrane preserving buffer (1 mM MgCl₂ and 0.1 mM CaCl₂ in PBS) at 37 °C with 5% CO₂ for 15 min to block nonspecific bindings. Thereafter, the blocking solution was discarded, the cells were washed with warm PBS four times, and the cultured medium was replaced with 2 mL of 10% FBS-supplemented MEM with or without CaCl₂, anti-ANXA1 mAb (IgG1), or isotype IgG1 as to divide these cells into 4 groups, including (i) control (normal culture without CaCl₂); (ii) high-calcium (with 20 mM CaCl₂),; (iii) high-calcium + anti-ANXA1 mAb (with 20 mM CaCl₂ and neutralization with 0.5 μ g/mL mouse monoclonal anti-ANXA1); and (iv) high-calcium + IgG1 (with 20 mM CaCl₂ and 0.5 μ g/mL IgG1, which was used as the isotype control of anti-ANXA1 mAb) (n = 3 per group). After 30 min of incubation at 37 °C with 5% CO₂, the cells were extensively washed again with warm PBS four times. COM crystal-cell adhesion was initiated by the addition of 10% FBS-supplemented MEM containing 100 µg/ mL COM crystals into each culture well. The cells were further incubated in a humidified incubator at 37 °C with 5% CO₂ for 30 min. Thereafter, the cells were vigorously washed by warm PBS

five times to remove unbound COM crystals. Finally, numbers of the adhered COM crystals, total cell numbers, and numbers of COM crystal-adhered cells were quantitated in at least 15 randomized high power fields (HPF) per culture well. Numbers of the adhered COM crystals were then normalized by total cell numbers and are presented as numbers of COM crystals per 100 cells (No./100 cells). Percentage of COM crystal-adhered cells (%) = [(number of COM crystal-adhered cells/total cell number) \times 100%]. All the experiments were performed in triplicate.

Cell Proliferation Assay

The degree of cell proliferation was determined by a conventional method using hemacytometer cell counting chamber. MDCK cells were prepared as for the above experiment to evaluate COM crystal-binding capacity. At the indicated time-points (24, 48, and 72 h after treatments), the cells were detached from the culture well using 0.1% trypsin in 2.5 mM EDTA and were immediately resuspended in 1 mL of FBS-containing MEM to terminate trypsin activity. Trypan blue staining was used to exclude dead cells and the numbers of viable cells were counted using hemacytometer. All the experiments were performed in triplicate.

Flow Cytometric Analysis of Cell Death (Annexin V/Propidium Iodide Costaining)

MDCK cells from the monolayer (including both adherent and floating cells) were trypsinized with 3 mL of 0.1% trypsin in 2.5 mM EDTA and resuspended in 10 mL of MEM. The harvested cells were centrifuged at 1500 rpm at 4 °C for 5 min and washed with PBS. Cell pellets were resuspended with annexin V buffer (10 mM HEPES, 140 mM NaCl ,and 2.5 mM CaCl₂·2H₂O; pH 7.4) at a final concentration of 5×10^5 cells/mL and then incubated with FITC-labeled annexin V (BD Biosciences; San Jose, CA), on ice for 15 min in the dark. Propidium iodide (BD Biosciences) was added into the samples at a final concentration of 10 μ L/mL prior to analysis. The cells were then analyzed by flow cytometry (FACScan, Becton Dickinson Immunocytometry System; San Jose, CA), and MDCK cells treated with 2 μ g/ mL camptothecin was used as a positive control. This experiment was performed in triplicate. Percentage of total cell death (% cell death) = [(number of both apoptotic and necrotic cells/number of all cells) \times 100%].

Evaluation of Wound Healing by Scratch Assay

Wound healing study by scratch assay was performed as described previously. ^{24,25} Briefly, MDCK cells were inoculated in a 6-well, polystylene plate (with lid) and maintained in the controlled or high-calcium medium as aforementioned. After 72 h of incubation with controlled or high-calcium culture medium, the cell monolayers were horizontally scratched along the culture well diameter using a 200 μ L plastic pipet tip to create a cell-free area. After gently washing with warm PBS to remove the debris and detached cells, the cultures were further maintained in the controlled or high-calcium medium at 37 °C with 5% CO₂. At the indicated time-points (0, 3, 6, 9, and 12 h after the scratch), each scratch wound was visualized for cellular morphological changes (from polygonal to spindle-shape with a loss of cell-to-cell contact) and multiple traveling waves (a well-known cellular behavior of wound healing) under a phase-contrast microscope and imaged by a digital camera. This image was submitted to Tarosoft Image framework v.0.9.6 (Nikon Corp.; Tokyo, Japan), which adopted to accurately measure the width of the wound (or cell-free width). All the experiments were performed in triplicate.

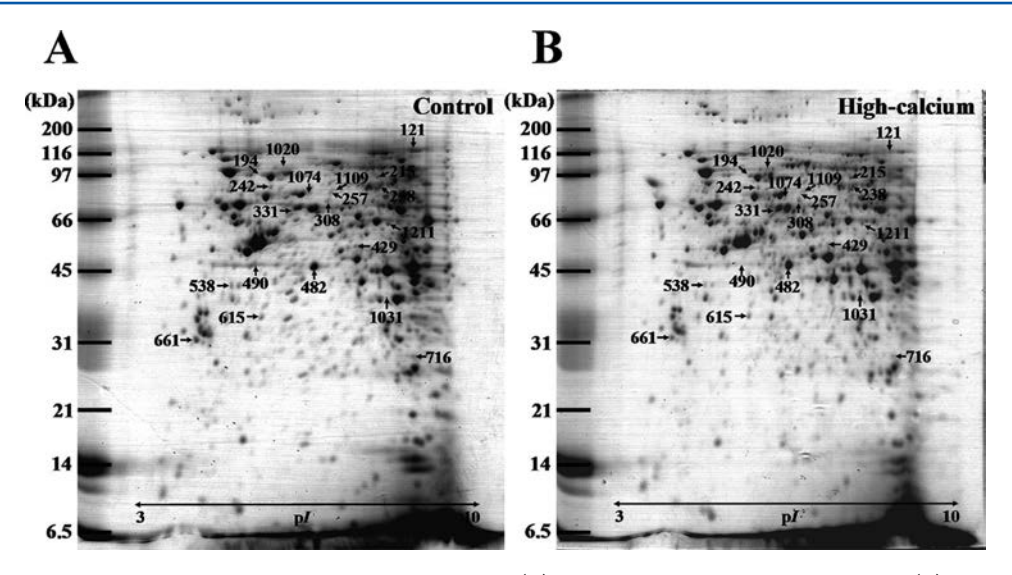


Figure 1. Representative 2-D gel images of proteins derived from controlled (A) and high-calcium-exposed MDCK cells (B). An equal amount of total protein $(200 \,\mu\text{g})$ derived from each sample was resolved by 2-DE using a pH gradient of 3–10 (nonlinear) for the IEF (first dimensional separation) and 12% SDS-PAGE for the second dimensional separation. The resolved protein spots were then visualized by SYPRO Ruby staining (n = 5 gels derived from 5 independent culture flasks for each group; a total of 10 gels were included for spot matching and quantitative intensity analysis). The differentially expressed protein spots with p < 0.05 were then identified by Q-TOF-MS and/or MS/MS analyses and are labeled with numbers (see also Table 1).

Statistical Analysis

The quantitative data are presented as mean \pm SEM. All statistical analyses were performed using SPSS software version 13.0 (SPSS; Chicago, IL). Comparisons of the data obtained from two sets of samples (i.e., control vs high-calcium) in all experiments (except for COM crystal-binding assay) were performed by unpaired Student's t test, whereas multiple comparisons by ANOVA were performed for COM crystal-binding assay. P values less than 0.05 were considered statistically significant.

RESULTS

Proteome Analysis

MDCK cells were maintained in the absence (control) or presence of 20 mM CaCl₂ (high-calcium) for 72 h. Thereafter, the controlled and high-calcium-exposed MDCK cells were harvested for protein extraction and were subjected to 2-DE analysis (n = 5 gels derived from 5 independent culture flasks per group). Spot matching revealed approximately 700 protein spots visualized in each 2-D gel. From these, quantitative intensity analysis and statistics revealed only 20 protein spots whose expression levels were significantly altered in the high-calciumexposed group (including 6 up-regulated proteins, 9 downregulated proteins, 1 protein that was detectable only after highcalcium exposure, and 4 proteins that were undetectable after high-calcium exposure) (Figure 1). These altered protein spots were subsequently identified using Q-TOF-MS and MS/MS analyses. Table 1 summarizes identification scores, spot intensities, and other related information of all the altered

Validation of Expression Proteomics Data by 2-D Western Blot Analysis

As summarized in Table 1, three forms of annexin A1 (ANXA1) (spot no. 482, 1031, and 1109) were up-regulated 1.39-, 20.60-, and 6.13-folds, respectively. The increase in these three forms of ANXA1 was validated by 2-D Western blot analysis using mouse monoclonal anti-ANXA1 as a primary antibody. In 2-D Western blot analysis, analytical procedures were similar to conventional

(1-D) Western blot analysis but used 2-DE to resolve the proteins prior to immunoblotting, instead of SDS-PAGE. The result clearly showed the increased levels of three forms of ANXA1 in the high-calcium-exposed cells (Figure 2), confirming the proteome data and mass spectrometric protein identification.

Protein Network Analysis and Subcellular Localization

Global protein network analysis using STRING 8.3 software²¹ was performed to gain functional significance of the altered proteins identified from expression proteomics study. All the altered proteins were submitted to STRING 8.3 to acquire three types of their expanded information, including functions, subcellular localizations, and interactions/associations with other identified proteins as well as noninputted proteins obtained from available databases and literatures. A successful map of protein association network with subcellular localization is shown in Figure 3, whereas Table 2 summarizes potential functions and subcellular localizations of individual proteins retrieved from UniProt (http://www.uniprot.org), EMBL-EBI (http://www.ebi.ac.uk), and/or PudMed (http://www.pubmed.org) databases.

From this protein network modeling, at least three potential functions were highlighted. First, up-regulation of calciumbinding protein (ANXA1) on apical surface of distal renal tubular cells may increase COM crystal-binding capability. Second, coordinated changes of up-regulation of antiproliferation protein (ANXA1) and down-regulation of proteins involved in protein synthesis (EEF1B2 and EEF1D), mitosis regulation (SEPT2), pre-mRNA processing (HNRPK), and cell proliferation (RUVBL1) suggested that the high-calcium-exposed MDCK cells had some defects in cell proliferation. Third, up-regulation of antimigration protein (ANXA1) and down-regulation of protein involved in wound healing (PGD) suggested that the high-calcium-exposed MDCK cells may have a defect in wound healing. All these hypotheses were subsequently addressed by several highly focused functional studies as follows.

Table 1. Summary of the Altered Proteins in MDCK Cells after Exposure to High-Calcium (Identified by Q-TOF-MS and/or MS/MS Analyses)^a

										intensity level (mean ± SEM)	mean ± SEM)		
	spot no.	protein name	NCBI entry	identified by	identification scores (MS, MS/ MS)	%Cov ^b (MS, MS/ MS)	no. of matched peptides (MS, MS/ MS)	Iq	MW (kDa)	control	high-calcium	ratio (high- calcium/ control)	P value
	Up-Reg	Up-Regulated Proteins											
	215	phosphoenolpyruvate carboxykinase 2, mitochondrial isoform 1	gil73962498	MS	112, NA	29, NA	18, NA	7.14	71.49	0.0905 ± 0.0110	0.1286 ± 0.0094	1.42	0.031
	238	apolipoprotein A-V	gil 126326986	MS	68, NA	30, NA	10, NA	7.02	59.04	0.0829 ± 0.0049	0.1089 ± 0.0101	1.31	0.049
	482	annexin A1	gil73946797	MS/MS	136, 199	57, 20	15, 4	5.84	38.89	0.8152 ± 0.0799	1.1349 ± 0.1069	1.39	0.044
	716	glutathione S-transferase, pi	gil57099635	MS, MS/ MS	78, 46	50, 5	8, 1	7.72	23.92	0.0633 ± 0.0265	0.1480 ± 0.0160	2.34	0.026
	1031	annexin A1	gil73946797	MS, MS/ MS	133, 84	8, 8	13, 2	6.97	39.14	0.0038 ± 0.0037	0.0779 ± 0.0136	20.60	0.001
	1109	annexin A1	gil73946797	MS	142, NA	56, NA	12, NA	5.84	38.89	0.0050 ± 0.0035	0.0312 ± 0.0081	6.13	0.019
	Down-l	Down-Regulated Proteins											
	242	heterogeneous nuclear ribonucleoprotein K	gil460789	MS, MS/ MS	84, 33	26, 2	11, 1	5.13	51.33	0.1089 ± 0.0084	0.0787 ± 0.0068	0.72	0.024
	257	ERO1-like protein alpha precursor	gil73963815	MS	90, NA	36, NA	14, NA	5.97	55.18	0.0609 ± 0.0045	0.0426 ± 0.0038	0.70	0.015
	308	ERO1-like protein alpha precursor	gil73963815	MS	76, NA	30, NA	10, NA	5.97	55.18	0.0879 ± 0.0215	0.0270 ± 0.0138	0.31	0.045
	331	RuvB-like 2	gil5730023	MS	91, NA	36, NA	12, NA	5.49	51.29	0.1304 ± 0.0105	0.0844 ± 0.0123	9.65	0.022
365	429	septin-2	gil73994331	MS, MS/ MS	117, 87	35, 7	17, 3	8.24	60.43	0.0779 ± 0.0038	0.0617 ± 0.0056	62:0	0.045
	538	elongation factor 1-delta isoform 3	gil73974686	MS/MS	NA, 77	NA, 17	NA, 2	4.94	30.33	0.0948 ± 0.0131	0.0559 ± 0.0046	0.59	0.024
	615	chloride intracellular channel protein 1	gil57094359	MS, MS/ MS	119, 44	54, 4	11, 2	5.18	27.35	0.1182 ± 0.0198	0.0354 ± 0.0161	0.30	0.012
	661	elongation factor 1-beta [$Homos piens$]	gil4503477	MS/MS	NA, 114	NA, 10	NA, 1	4.50	24.92	0.2486 ± 0.0115	0.1518 ± 0.0299	0.61	0.017
	1074	glutamine-fructose-6-phosphate aminotransferase	gil 126304009	MS	71, NA	23, NA	10, NA	60.9	77.93	0.0819 ± 0.0132	0.0395 ± 0.0067	0.48	0.021
d	Protein	Protein That Was Detectable Only after High-Calcium Exposure	alcium Exposur	е									
	1020	CASP8 and FADD-like apoptosis regulator precursor	gil 148283492	MS	69, NA	32, NA	9, NA	6.38	55.98	0.0000 ± 0.0000	0.0436 ± 0.0120	Divided by 0	0.007
/10	Protein.	Proteins That Were Undetectable after High-Calcium Exposure	Icium Exposure										
1021/p	121	transient receptor potential cation channel, subfamily M, member 6	gil 119582957	MS	75, NA	19, NA	10, NA	8.67	92.59	0.1076 ± 0.0297	0.0000 ± 0.0000	0.00	0.007
	194	lamin B1	gil 296485609	MS	78, NA	12, NA	25, NA	5.35	62.22	0.0355 ± 0.0149	0.0000 ± 0.0000	0.00	0.044
	490	unidentified	NA	NA	NA, NA	NA, NA	NA, NA	NA	NA	0.0375 ± 0.0109	0.0000 ± 0.0000	0.00	0.009
Proteom	1211	6-phosphogluconate dehydrogenase, decarboxylating isoform 1	gil73950940	MS	69, NA	29, NA	10, NA	9.99	53.58	0.0578 ± 0.0218	0.0000 ± 0.0000	0.00	0.029

 $^{a}NA = not \text{ applicable. }^{b}\%Cov = \% \text{ sequence coverage [(number of matched residues)/(total number of residues in the entire sequence)} \times 100\%].$

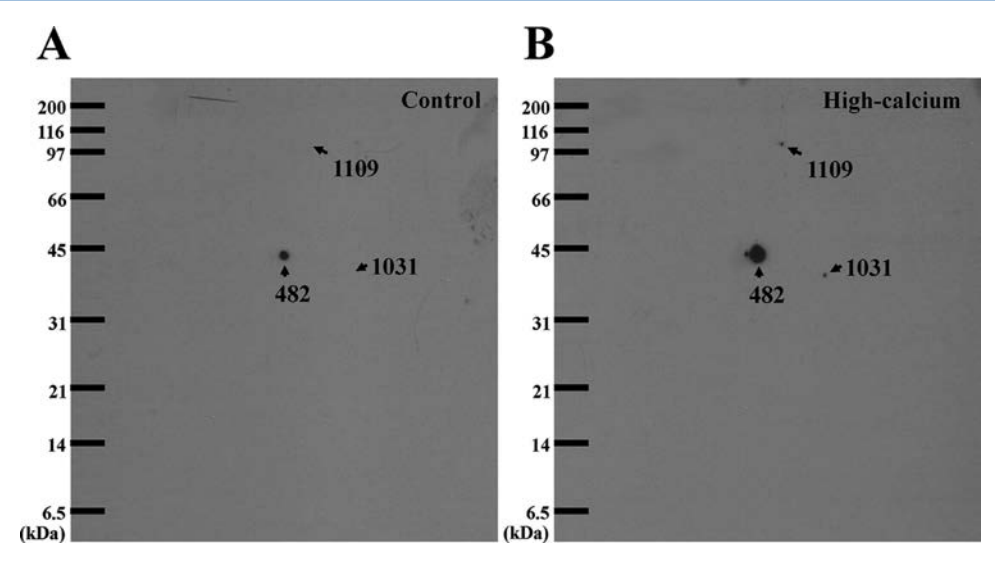


Figure 2. 2-D Western blot analysis of ANXA1. Proteins derived from the controlled and high-calcium-exposed MDCK cells (with an equal amount of 100 μ g total protein) were resolved with 2-DE and transferred onto nitrocellulose membranes. Proteins on the membranes were then examined by Western blot analysis using mouse monoclonal anti-ANXA1 as a primary antibody and rabbit antimouse IgG conjugated with HRP as a secondary antibody. Immunoreactive spots were then visualized by chemiluminescence and autoradiography. Spot no. 482, 1031, and 1109 corresponded to the three forms of ANXA1 that were markedly increased in the high-calcium-expose cells (see also Figure 1 and Table 1).

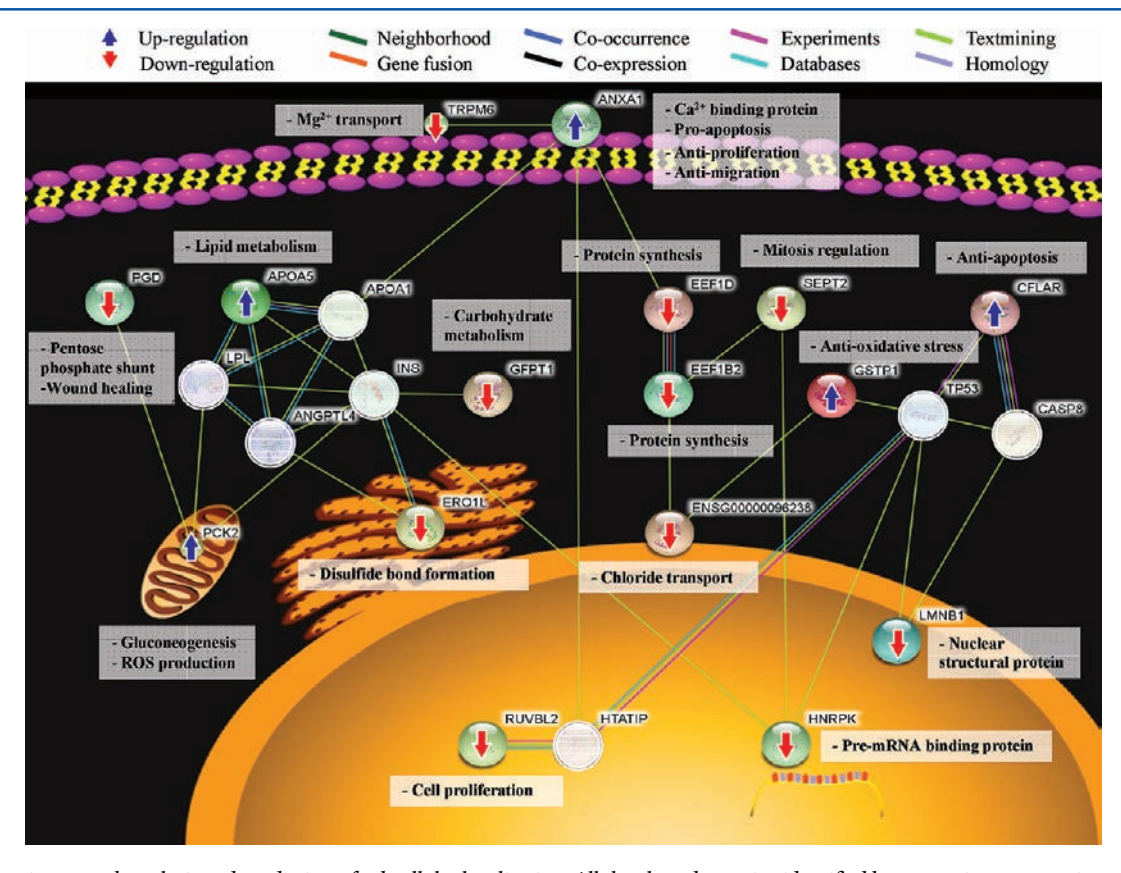


Figure 3. Protein network analysis and prediction of subcellular localization. All the altered proteins identified by expression proteomics approach were submitted to STRING 8.3. The inputted proteins, which were identified as the significantly altered proteins, are demonstrated as the colored nodes, whereas those curated from protein database and literatures are designated as the white nodes. Each line represents a specific type of association between protein nodes. Up-regulation and down-regulation of each protein is labeled with upward and downward arrows, respectively.

Validation of the Increased Surface Expression of ANXA1 at Apical Membranes

From protein network analysis and prediction of subcellular localization, the increase in ANXA1, which is a calcium-binding protein, might be localized at apical membranes of renal tubular

cells and related to the increased COM crystal-binding capacity. Although 2-D Western blot analysis successfully confirmed the increase of ANXA1 in the high-calcium-exposed cells (Figure 2), this data did not address subcellular localization of such increase (because whole cell lysate was used). To address this issue, apical

Table 2. Functional Roles and Subcellular Localizations of the Identified Altered Proteins and the Interacting Proteins Predicted by the Protein Association Network Modeling

gene name	protein name	function(s)	subcellular localization
Up-Regulated Protein	as		
ANXA1	annexin A1	calcium binding; Antiproliferation; pro-apoptosis; Antimigration	plasma membrane; cytoplasm; nucleus
APOA5	apolipoprotein A-V	lipid metabolism	cytoplasm
CFLAR	CASP8 and FADD-like apoptosis regulator precursor	antiapoptosis	cytoplasm
GSTP1	glutathione S-transferase P	antioxidant enzyme	cytoplasm
PCK2	phosphoenolpyruvate carboxykinase, mitochondrial isoform	gluconeogenesis; involved in oxidative stress	mitochondria
Down-Regulated Prot	teins		
ENSG00000096238	chloride intracellular channel protein 1	pH-dependent chloride ion channel	nuclear membrane
EEF1D	elongation factor 1-delta	protein biosynthesis	cytoplasm
EEF1B2	elongation factor 1-beta	protein biosynthesis	cytoplasm
ERO1L	endoplasmic oxidoreductin-1-like protein	disulfide bond formation	endoplasmic reticulum
GFPT1	glucosamine-fructose-6-phosphate aminotransferase 1	carbohydrate metabolism	cytoplasm
HNRPK	heterogeneous nuclear ribonucleoprotein K	major pre-mRNA binding protein	nucleus
LMNB1	lamin B-1	nuclear structural protein	nuclear membrane
PGD	6-phosphogluconate dehydrogenase, decarboxylating	pentose phosphate shunt; Involved with wound healing	cytoplasm
RUVBL2	RuvB-like protein 2	cell proliferation	nucleus
SEPT2	septin-2	mitosis regulation	cytoplasm
TRPM6	transient receptor potential melastatin 6	magnesium (and calcium) transport	plasma membrane
Predicted Interacted 1	Proteins Whose Abundance Levels Were Unknown		
ANGPTL4	angiopoietin-related protein 4	antiproliferation; Antimigration	cytoplasm
APOA1	apolipoprotein A-I	lipid metabolism	cytoplasm
CASP8	Caspase 8	Pro-apoptosis	cytoplasm
HTATIP	histone acetyltransferase HIV-1 Tat interactive protein	gene transcription	nucleus
LPL	lipoprotein lipase	lipid degradation	secreted protein
INS	insulin	glucose metabolism	secreted protein
TP53	tumor suppressor p53	antiproliferation; pro-apoptosis	cytoplasm

membranes were isolated from the cells using a peeling method described recently.²² The purity of this isolation was confirmed by evaluations of markers for apical (gp135) and basolateral (Na +/K+-ATPase-α1) membranes.²² Thereafter, the apical membrane fraction was subjected to 1-D Western blot analysis for ANXA1 comparing between controlled and high-calcium conditions. The data confirmed that, first, ANXA1 was present in apical membranes and that, second, apical membrane ANXA1 was significantly increased in the high-calcium-exposed cells as compared to the controls (Figure 4A). Additionally, the cytosolic fraction was also collected and subjected to 1-D Western blot analysis for ANXA1. The data demonstrated that, first, two ANXA1 isoforms in cytosolic fraction had lower molecular masses as compared to the one found in apical membrane fraction and that, second, these two ANXA1 isoforms found in cytosolic fraction were also increased in the high-calciumexposed cells as compared to the controls (Figure 4A). Taken together, the increases in all three isoforms of ANXA1 found in both apical and cytosolic fractions by 1-D Western blot analysis were consistent to the findings observed by proteomic analysis (Figure 1 and Table 1) and 2-D Western blot analysis (Figure 2).

The increase in apical membrane expression of ANXA1 in the high-calcium-exposed cells was also confirmed by laser-scanning confocal microscopy. The cells were labeled with primary antibody (anti-ANXA1 mAb) without permeabilization to avoid interfering staining of the intracellular compartment (another localization of ANXA1). The immunofluorescence data nicely confirmed that the apical membrane expression of ANXA1 was

markedly increased in the high-calcium-exposed cells (Figure 4B).

COM Crystal-Binding Capacity and the Effect of Neutralization by Anti-ANXA1 mAb

The increase of ANXA1 levels on apical surface of distal renal tubular cells may exert some important roles in the pathogenic mechanisms of COM nephrolithiasis, particularly COM crystalbinding capacity. Our hypothesis that the increased expression of ANXA1 on apical surface could enhance COM crystal-binding capacity was then addressed. After 72 h of incubation with or without 20 mM CaCl₂, the culture medium was replaced with 10% FBS-supplemented MEM with or without CaCl₂, anti-ANXA1 mAb, or IgG1 as described in the materials and methods section. After 30 min of incubation, the cells were then treated with 100 μ g/mL COM crystals for 30 min. Thereafter, the cells were vigorously washed using PBS five times to remove unbound COM crystals. Finally, numbers of the adhered COM crystals were quantitatively analyzed in triplicate. The data showed a significantly greater number of the adhered COM crystals on the surface of the high-calcium-exposed cells as compared to the controls (Figure 5). Neutralization with anti-ANXA1, not IgG1 isotype control, could reduce the number of adhered crystals to the basal levels (Figure 5).

Cell Proliferation Assay and Quantitative Analysis of Cell Death

Morphological examination during the cell maintenance and the proposed functional changes by protein network modeling

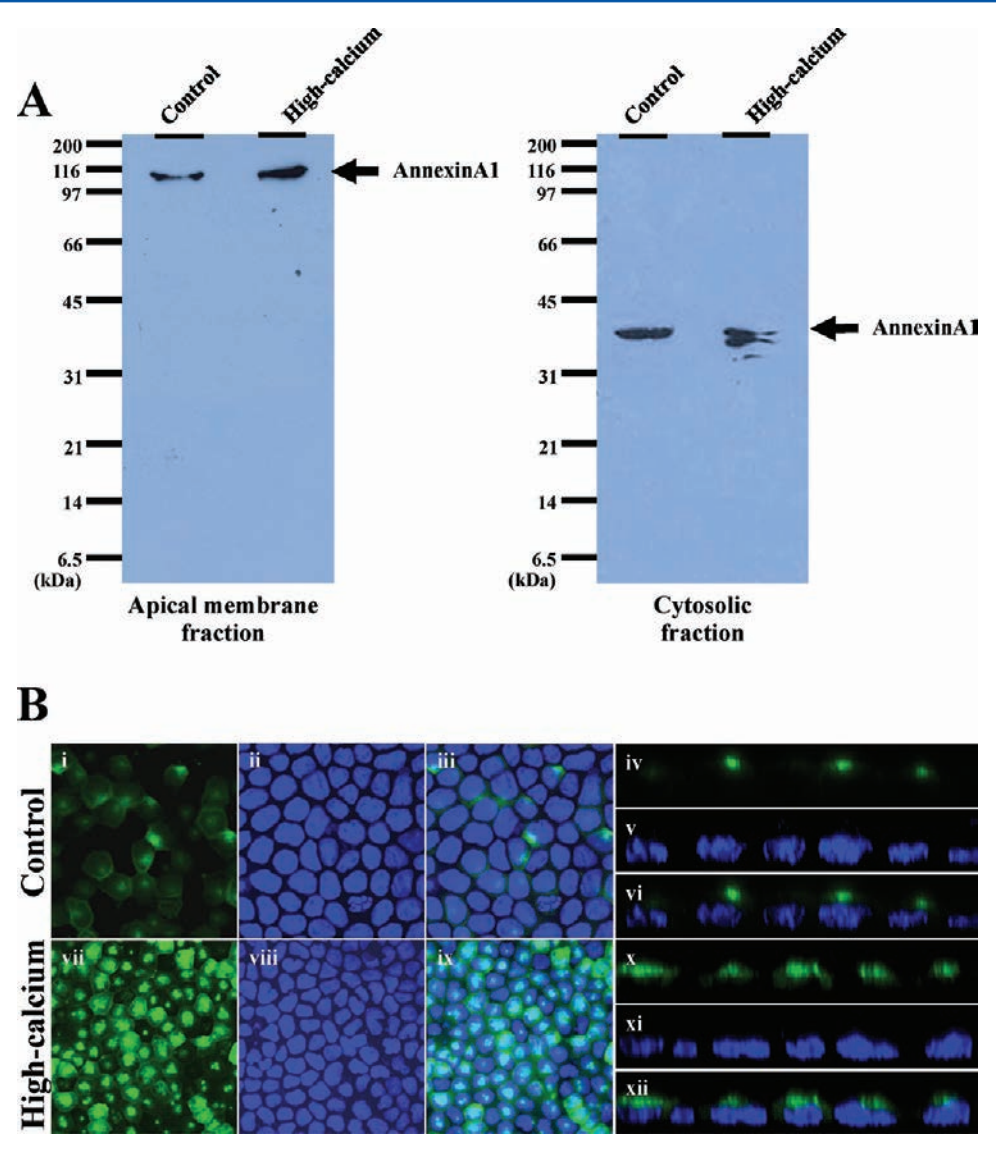


Figure 4. Validation of the increased surface expression of ANXA1 at apical membranes of the high-calcium-exposed cells. (A) 1-D Western blot analysis of apical membrane and cytosolic fractions was performed using mouse monoclonal anti-ANXA1 as a primary antibody and rabbit antimouse IgG conjugated with HRP as a secondary antibody. Immunoreactive bands were then visualized by chemiluminescence and autoradiography. (B) Surface expression of ANAXA1 on apical membranes was also evaluated by immunofluorescence staining and laser-scanning confocal microscopy. ANXA1 is presented in green, whereas nuclei are presented in blue (Hoechst dye). Panels (i–iii) and (vii–ix) show the top view, whereas panels (iv–vi) and (x–xii) illustrate the sagittal sections. Original magnification power was $630\times$ in all panels.

(Figure 3) suggested that the high-calcium-exposed cells might have a defect in cell proliferation. To address this hypothesis, the total numbers of MDCK cells (which reflected the degree of cell proliferation) in the controlled and high-calcium-exposed conditions were serially evaluated at 24, 48, and 72 h after the treatment. The data showed that the high-calcium-exposed cells had significant decreases in the total cell numbers (approximately 50.9 ± 12.7 , 42.9 ± 11.5 , and $42.0 \pm 4.5\%$ decreases compared to those of controls at 24, 48 and 72 h post-treatment, respectively) (Figure 6A). However, one might argue that the reduction of total cell numbers might be from cytotoxicity of high-calcium as there were changes in some proteins involved in cytotoxicity. We thus performed quantitative analysis of cell death using flow cytometry and annexin V/propidium iodide co-staining to measure both cell apoptosis and necrosis. The cell death assay revealed comparable percentages of apoptotic and necrotic cells as well as total cell death (5.05 ± 0.31 vs $5.07 \pm 0.85\%$ for control vs high-calcium; P = 0.971) in both conditions (Figure 6B),

implicating that the reduction of total cell numbers was from impaired cell proliferation, not from the cytotoxicity of high-calcium.

Evaluation of Wound Healing by Scratch Assay

Another functional abnormality of the high-calcium-exposed cells highlighted from the protein network modeling was the defect in wound healing. To address this functional abnormality, the artificial wounds were created on the confluent monolayer of the controlled and high-calcium-exposed cells. These scratched wounds had sharp-edge and the width of the wound (or cell-free width) (measured immediately after the scratch) was highly consistent (approximately 649.1 \pm 8.9 μ m from 18 independent experiments; coefficient of variation or CV = 1.37%). Wound healing capability of the controlled and high-calcium treated cells were then evaluated at various time-points by morphological examination and quantitative measurement of cell-free width. In the controlled condition, the cells localized at the scratched edges

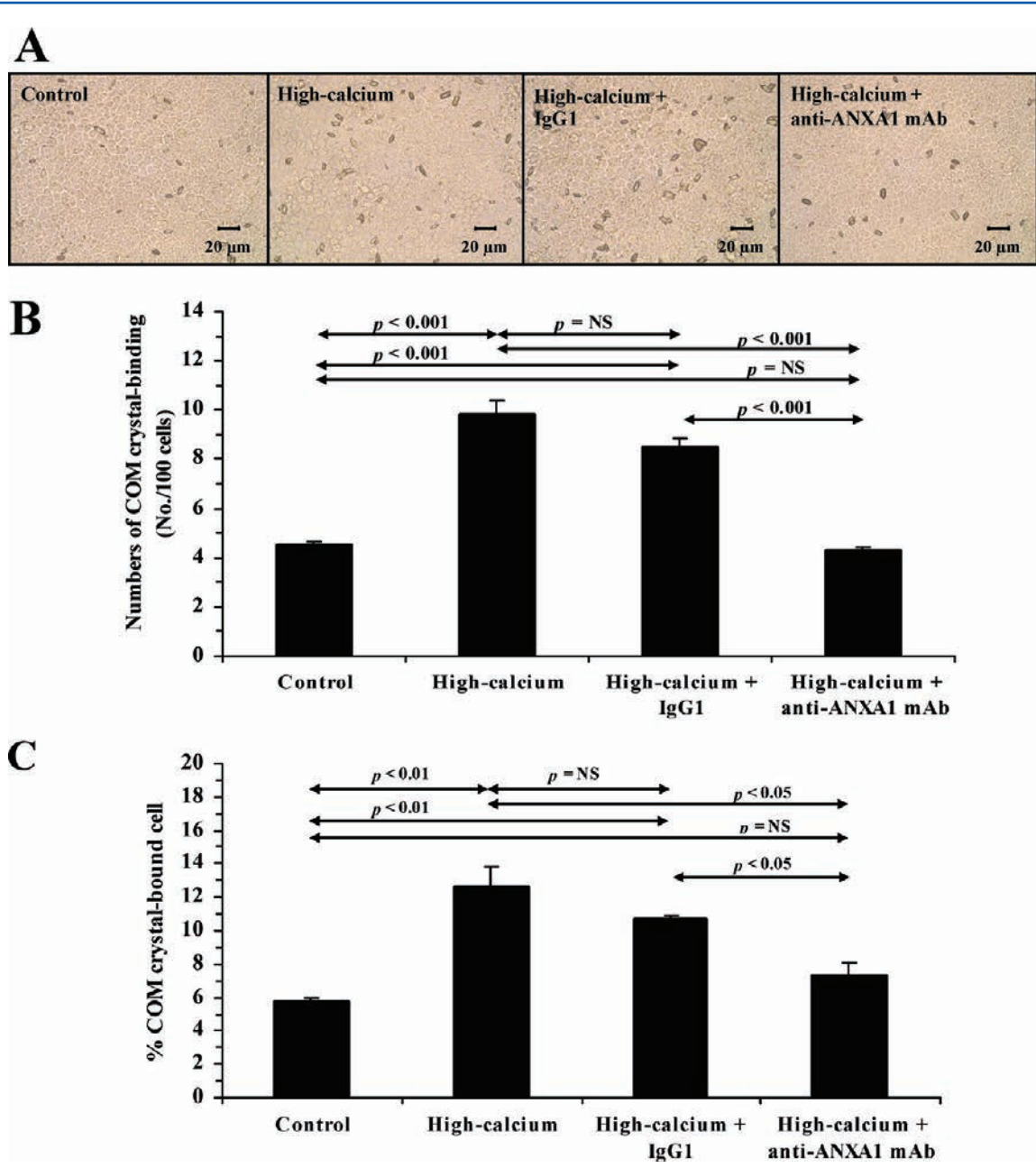


Figure 5. COM crystal-binding capacity and the effect of neutralization by anti-ANXA1 mAb. (A) Phase-contrast microscopic examination of 4 groups of cells, including (i) control (normal culture without $CaCl_2$); (ii) high-calcium (with 20 mM $CaCl_2$); (iii) high-calcium + anti-ANXA1 mAb (with 20 mM $CaCl_2$ and neutralization with 0.5 μ g/mL mouse monoclonal anti-ANXA1); and (iv) high-calcium + IgG1 (with 20 mM $CaCl_2$ and 0.5 μ g/mL IgG1, which was used as the isotype control of anti-ANXA1 mAb) (n=3 per group). Original magnification power was 400× for all panels. (B) Quantitative analysis of the adhered COM crystals in individual groups per 100 cells (no./100 cells). (C) Percentage of COM crystal-adhered cells (%). The data of each bar is presented as mean \pm SEM of three independent experiments. * = P < 0.0001 versus the control condition. NS = not statistically significant.

had morphological changes and gradually migrated to the cell-free area, starting at 3 h postscratching (Figure 7A). In the high-calcium condition, these morphological changes and cell migration required a longer time to develop (starting at 6 h postscratching). At 12 h postscratching, the wounds in the controlled condition were successfully closed by the migratory cells, whereas the wounds in the high-calcium-exposed condition remained unclosed (Figure 7A). Quantitative measurement of the cell-free widths also confirmed the delay or impairment of wound healing in the high-calcium-exposed cells as demonstrated by significantly greater cell-free widths in the high-

calcium-exposed cells compared to the controls at all time-points (Figure 7B).

DISCUSSION

Hypercalciuria is the most common metabolic cause of COM nephrolithiasis^{1,3–5} and can also lead to impaired renal tubular function. However, cellular responses of distal renal tubular cells to the hypercalciuric state remained largely unknown. We therefore performed a gel-based proteomics study to identify altered proteins in distal renal tubular cells in response to high-calcium exposure (Figure 1 and Table 1). These altered proteins were involved in several cellular functions,

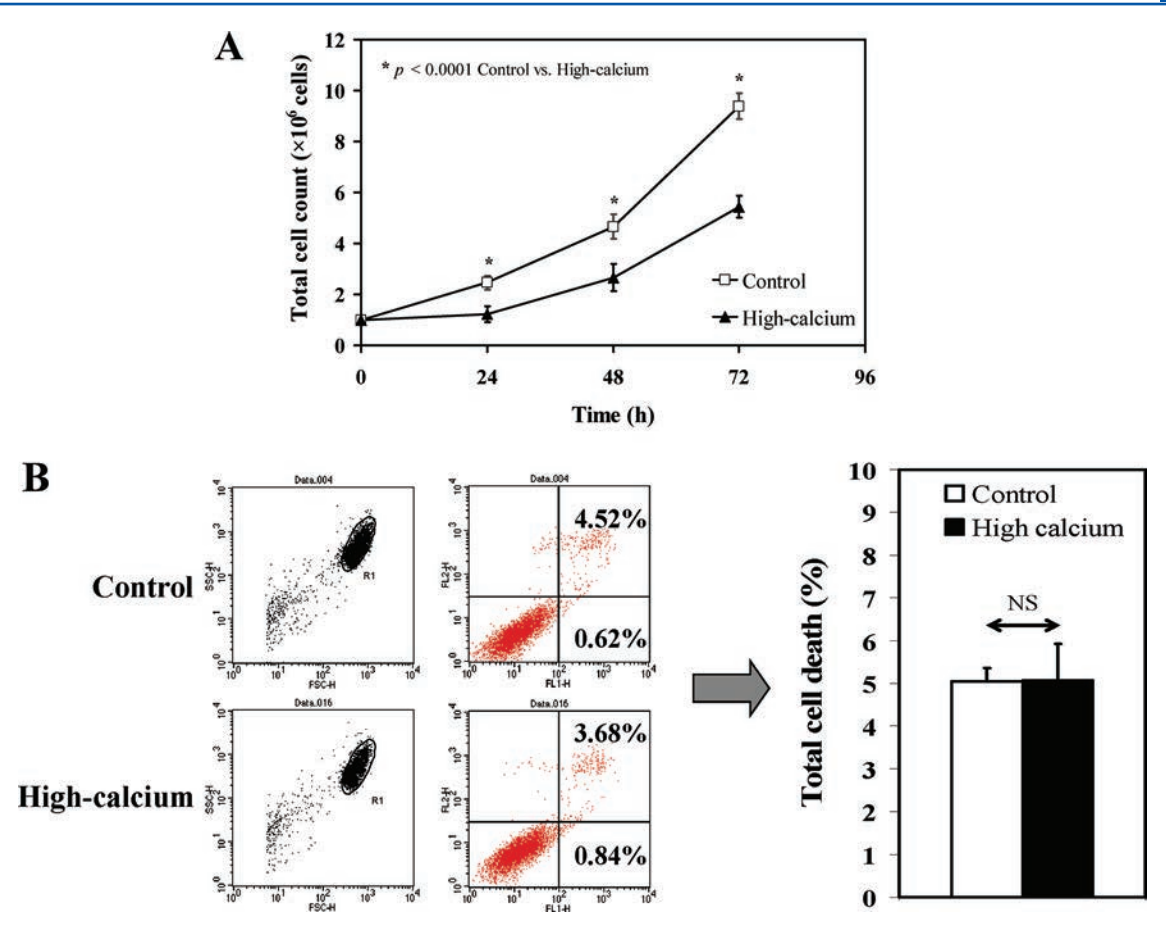


Figure 6. Cell proliferation assay (A) and quantitative analysis of cell death (B). (A) At 24, 48, and 72 h post-treatment, the cells were detached from the culture well using 0.1% trypsin in 2.5 mM EDTA and were immediately resuspended in 1 mL of FBS-containing MEM to terminate trypsin activity. Trypan blue staining was used to exclude dead cells, and the numbers of viable cells were counted using hemacytometer. (B) After 72 h of incubation, both controlled and high-calcium-treated cells were examined for percentage of the total cell death using flow cytometry with annexin V and propidium iodide co-staining. All the quantitative data are presented as mean \pm SEM of three independent experiments. * = P < 0.0001 versus the control condition. NS = not statistically significant.

including calcium binding, protein synthesis, carbohydrate metabolism, lipid metabolism, cell proliferation, mitosis regulation, apoptosis, cell migration, oxidative stress, and ion transport (Table 2). After identification of these altered proteins, protein network analysis (Figure 3) and several highly focused functional studies (Figures 4–7) were sequentially performed to address functional significance of the expression proteomics data.

Protein network analysis using STRING 8.3 was very useful as this bioinformatic tool provided several important aspects to further design highly focused functional studies. These included potential functions of the altered proteins, their subcellular localizations, protein—protein interactions, and the involved biological processes/pathways to create new hypotheses. In our present study, several hypotheses were guided from protein association network analysis including:

Hypothesis I: The expression proteomics data and prediction of subcellular localization and cellular function suggested that ANXA1 was up-regulated on apical surface of renal tubular cells upon exposure to high-calcium and might promote COM crystal-cell adhesion.

Hypothesis II: The coordinated changes of up-regulation of antiproliferative protein (ANXA1) and down-regulation of proteins involved in cell proliferation (RUVBL2), mitosis regulation (SEPT2), mRNA processing (HNRPK), and protein biosynthesis (EEF1B2 and

EEF1D) strongly suggested that renal tubular cells under the high-calcium condition had a defect in cell proliferation.

Hypothesis III: The coordinated changes of up-regulation of antimigration protein (ANXA1) and down-regulation of protein involved in wound healing (PGD) suggested that the high-calcium-exposed cells had a defect in epithelial wound healing.

It seemed that ANXA1 played pivotal roles in high-calcium-induced changes in renal tubular cells as this protein was involved in all of these hypotheses. This was probably due to its multiple biological functions, including calcium- and phospholipid-binding activity, inhibition of cell proliferation and migration, anti-inflammation, and immunological regulation. Therefore, we first confirmed the expression proteomics data by 2-D Western blot analysis (Figure 2), which demonstrated upregulation of three forms of ANXA1, consistent to the proteomic data. Finally, all of the aforementioned hypotheses were addressed and indeed confirmed by several highly focused functional studies as follows.

Validation of Hypothesis I resulted in the identification of ANXA1, a calcium-binding protein, as a novel COM crystal-binding molecule on apical surface of renal tubular cells (Figure 5). From expression proteomics data, up-regulation of ANXA1 in high-calcium-exposed MDCK cells implicated that this protein is

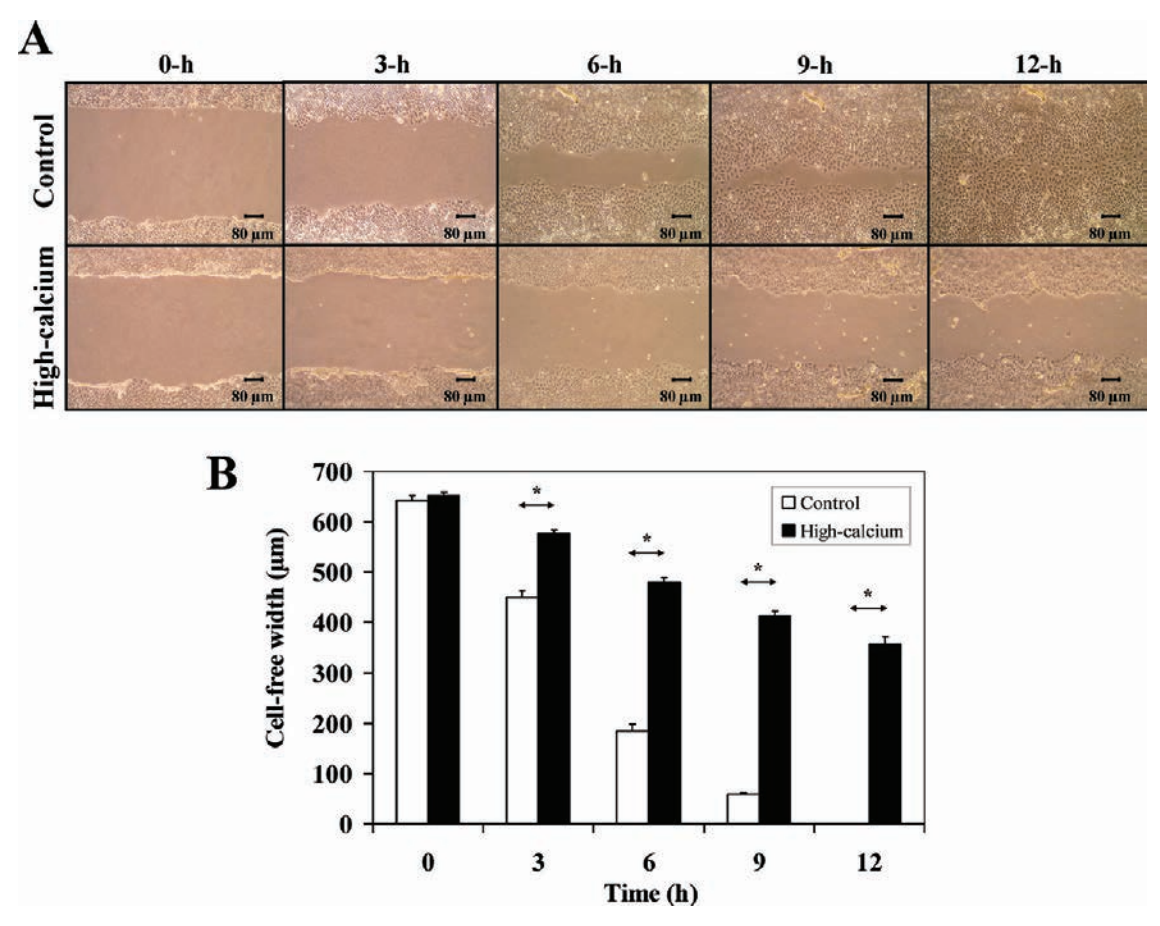


Figure 7. Evaluation of wound healing by scratch assay. After 72 h of incubation, artificial wounds were created on the confluent monolayers of the controlled and high-calcium-exposed cells. At the indicated time-points, these wounds were imaged by phase contrast microscopy (A) and the cell-free widths were measured and analyzed by Tarosoft Image framework v.0.9.6 software (B). All the quantitative data are presented as mean \pm SEM of three independent experiments. * = P < 0.0001 versus the control condition. In all panels of part A, original magnification power was $100 \times$.

involved in COM kidney stone formation. This proposed role of ANXA1, however, would be reasonable only if this protein was expressed on the apical membranes of renal tubular cells (in addition to its well-known locale in cytoplasm). Although 2-D Western blot analysis confirmed the expression proteomics data, it did not provide subcellular localization of the change. We therefore isolated apical membranes and confirmed that ANXA1 was also expressed at apical membranes of renal tubular cells and was up-regulated when the cells were exposed to high-calcium (Figure 4). This solid data led to a further hypothesis that the upregulation of this calcium-binding protein (ANXA1) on the cell surface would result to the enhanced COM crystal-binding capacity of the high-calcium-exposed cells. The latter was nicely confirmed by COM crystal-binding assay, which demonstrated that the high-calcium-exposed cells had increased COM crystalbinding capacity and neutralization by anti-ANXA1, not its isotype control (IgG1), successfully prevented this enhancement (Figure 5). ANXA1 has been extensively studied for its clinical applications in several malignancies, ^{28–30} inflammation, ^{31,32} neuroendocrine, ³³ and antinociception. ³⁴ A recent study by Thurgood et al.³⁵ has demonstrated that ANXA1 was a common constituent of calcium oxalate dihydrate (COD) crystals, which were crystallized in the human urine. However, its functional significance in COM kidney stone disease remained unclear. Our present study provided functional evidence demonstrating that ANXA1 on apical surface of distal renal tubular cells could serve

as the COM crystal receptor and may play a crucial role in COM stone formation.

Validation of Hypothesis II revealed that proliferation of renal tubular cells was suppressed by the high-calcium environment (Figure 6A), whereas the effect of cell death on the reduced numbers of the cells was excluded by quantitative analysis of cell death using flow cytometry with annexin V/propidium iodide costaining, which demonstrated that both apoptotic and necrotic cell death were not increased by high-calcium (Figure 6B). This functional defect in cell proliferation was confidently proposed from the strong interactions/associations of ANXA1, RUVBL2, SEPT2, HNRPK, EEF1B2, and EEF1D (Figure 3). ANXA1 seemed to play a major role in this subset of protein network. ANXA1 is well characterized as a regulator of the antiproliferative process by blocking epidermal growth factor (EGF)-mediated cell proliferation, activating extracellular signal-regulated kinase (ERK)-mediated disruption of actin cytoskeleton, and inhibiting cyclin D1.^{27,36} Antiproliferative activity of ANXA1 is localized at its N-terminus since this part of the peptide fragment significantly inhibits growth and proliferation of A549 lung cancer cells in vitro.³⁷ The antiproliferative activity of ANXA1 has been demonstrated also in clinical cancer tissues,²⁷ and down-regulation of ANXA1 has been observed in several cancer types; e.g., esophageal squamous cell carcinoma, ³⁸ prostatic adenocarcinoma, ³⁹ and bladder cancer, ⁴⁰ as cancer cells attempt to suppress antiproliferative proteins to exhibit their tumorigenic properties.²⁷ The coordinated down-regulation of proteins

involved in cell proliferation (RUVBL2), mitosis regulation (SEPT2), mRNA processing (HNRPK), and protein biosynthesis (EEF1D and EEF1B2) were then considered as the downstream effectors of antiproliferative effect of ANXA1 because most of these proteins are involved in the common pathway of cell proliferation machinery.

Validation of Hypothesis III revealed that renal tubular cells under high-calcium environment had a significant defect in wound healing (Figure 7). This hypothesis was confidently proposed from the coordinated changes of ANXA1 and PGD in the high-calcium-exposed cells. ANXA1 was presumably contributed to the defective wound healing process by its antimigration activity. Several previous studies have demonstrated that ANXA1 could inhibit migration of several cell types in vitro and in vivo⁴¹⁻⁴³ via the activation of formyl peptide receptor (FPR).44 Another player in this functional defect was PGD, which plays an important role in the pentose phosphate shunt and has been reported to be associated with wound healing capability. 45,46 An argument might be raised that the impaired cell proliferation might be responsible for (or contribute to) the defective wound healing. It is known that wound healing is the result of overlapping processes of cell proliferation and migration. Nevertheless, it seems that the impaired cell migration plays more dominant role during the acute phase response of wound healing. ^{24,25} This concept has been strongly supported by the study of Storesund et al.,²⁵ which demonstrated that wound healing capacity of normal oral keratinocytes in the presence of trefoil factor 3 was not affected by mitomycin C, a potent inhibitor of cell proliferation, but was markedly affected by cytochalasin B, a potent inhibitor of cell migration. Hence, we believe that the impaired migration was the major cause of the defective wound healing although the impaired cell proliferation could not be entirely excluded. The defect in wound healing of the high-calcium-exposed cells may implicate some aspects of renal tubular impairment caused by hypercalciuria. $^{10-15}$ As the cells lose their regeneration capacity, renal tubules may be unable to fully restore their structures and/or functions after exposure to the noxious stimuli.

It should be noted that, first, although MDCK cells represent mainly distal renal tubular cells, several lines of evidence have suggested that these cells also represent some features of collecting duct cells. ^{47,48} Buchholz et al. ⁴⁷ used MDCK cells as the model for principal and alpha-intercalated cells of collecting duct to demonstrate cystogenesis and cyst growth in response to cAMP and ATP signaling, whereas Dos Santos, et al. ⁴⁸ showed that MDCK cells could respond to aldosterone (a hormone that stimulated H⁺ secretion by intercalated cells of collecting duct) through a genomic pathway in order to enhance vacuolar H⁺-ATPase activity. Therefore, effects of high-calcium on MDCK cells observed in the present study reflected not only pathophysiologic changes in distal renal tubular cells but also (although partially) some phenomena in renal collecting duct.

Second, an addition of 20 mM CaCl₂ to the culture medium could increase the osmolarity up to approximately 15% of the basal level (data not shown). Thus, effects of increased osmolarity should be taken into account. Further studies are required to differentiate effects of high-calcium from those of increased osmolarity. Finally, our data may be applicable to kidney stones that are originated from the intratubular luminal site but not applicable to kidney stones that are originated from the interstitial site (Randall's plaque)^{49,50} of which pathogenic mechanisms differ.

In summary, our present study revealed pathophysiological responses of MDCK cells upon 72 h of exposure to the highcalcium environment. These changes may, at least in part, explain the common complications occurred in hypercalciuric patients, including COM kidney stone formation and renal tubular impairment. Our in vitro study offers several candidates for further targeted studies to confirm their relevance in hypercalciuria and kidney stone disease in vivo. According to the involvements of ANXA1 observed in vitro, it is speculated that this multifunctional protein may serve as a central regulator in hypercalciuric complications by enhanced COM crystal-binding capacity, impaired cell proliferation, and impaired wound healing. Therefore, ANXA1 may be considered as a novel drug target for preventing kidney stone formation complicated by hypercalciuria. Finally, our present study also demonstrated that a classical proteomics approach (starting from expression proteomics followed by bioinformatic analysis) can be used to obtain additional and very important data to generate new hypotheses, which can then be addressed by highly focused functional studies. This is thus the ideal approach for unraveling the pathogenic mechanisms and pathophysiology of diseases as well as for defining novel therapeutic targets.

ASSOCIATED CONTENT

S Supporting Information

Supplementary methods. This material is available free of charge via the Internet at http://pubs.acs.org.

AUTHOR INFORMATION

Corresponding Author

*Phone/Fax: +66-2-4184793. E-mail: thongboonkerd@dr.com or vthongbo@yahoo.com.

Notes

The authors declare no competing financial interest.

ACKNOWLEDGMENTS

We are grateful to Professor Shui-Tein Chen and Dr. Supachok Sinchaikul for their technical support on mass spectrometric analyses. This study was supported by the Office of the Higher Education Commission and Mahidol University under the National Research Universities Initiative, and The Thailand Research Fund (RTA5380005) to V.T. K.F. and P.P. are supported by the Royal Golden Jubilee Ph.D. Program of The Thailand Research Fund, whereas V.T. is also supported by the "Chalermphrakiat" Grant, Faculty of Medicine, Siriraj Hospital.

ABBREVIATIONS USED

ANGPTL4, angiopoietin-related protein 4; ANXA1, annexin A1; APOA1, apolipoprotein A-I; APOA5, apolipoprotein A-V; CASP8, caspase 8; CFLAR, CASP8 and FADD-like apoptosis regulator; ENSG00000096238, chloride intracellular channel protein 1; EEF1B2, elongation factor 1-beta; EEF1D, elongation factor 1-delta; ERO1L, endoplasmic oxidoreductin-1-like protein; GFPT1, glucosamine-fructose-6-phosphate aminotransferase 1; GSTP1, glutathione S-transferase Pi; HNRPK, heterogeneous nuclear ribonucleoprotein K; HTATIP, histone acetyltransferase; INS, insulin; LMNB1, lamin B-1; LPL, lipoprotein lipase; PCK2, phosphoenolpyruvate carboxykinase, mitochondrial isoform; PGD, 6-phosphogluconate dehydrogenase, decarboxylating; RUVBL2, RuvB-like protein 2; SEPT2,

septin-2; TP53, tumor suppressor p53; TRPM6, transient receptor potential melastatin 6

REFERENCES

- (1) Liebman, S. E.; Taylor, J. G.; Bushinsky, D. A. Idiopathic hypercalciuria. *Curr. Rheumatol. Rep.* **2006**, *8*, 70–75.
- (2) Vezzoli, G.; Soldati, L.; Gambaro, G. Update on primary hypercalciuria from a genetic perspective. *J. Urol.* **2008**, *179*, 1676–1682.
- (3) Worcester, E. M.; Coe, F. L. New insights into the pathogenesis of idiopathic hypercalciuria. *Semin. Nephrol.* **2008**, *28*, 120–132.
- (4) Worcester, E. M.; Coe, F. L. Nephrolithiasis. *Prim. Care* **2008**, 35 (vii), 369–391.
- (5) Lerolle, N.; Lantz, B.; Paillard, F.; Gattegno, B.; Flahault, A.; Ronco, P.; Houillier, P.; Rondeau, E. Risk factors for nephrolithiasis in patients with familial idiopathic hypercalciuria. *Am. J. Med.* **2002**, *113*, 99–103.
- (6) Asplin, J. R.; Parks, J. H.; Coe, F. L. Dependence of upper limit of metastability on supersaturation in nephrolithiasis. *Kidney Int.* **1997**, *52*, 1602–1608.
- (7) Lieske, J. C.; Farell, G.; Deganello, S. The effect of ions at the surface of calcium oxalate monohydrate crystals on cell-crystal interactions. *Urol. Res.* **2004**, *32*, 117–123.
- (8) Rabinovich, Y. I.; Daosukho, S.; Byer, K. J.; El Shall, H. E.; Khan, S. R. Direct AFM measurements of adhesion forces between calcium oxalate monohydrate and kidney epithelial cells in the presence of Ca²⁺ and Mg²⁺ ions. *J. Colloid Interface Sci.* **2008**, 325, 594–601.
- (9) Curhan, G. C.; Willett, W. C.; Speizer, F. E.; Stampfer, M. J. Twenty-four-hour urine chemistries and the risk of kidney stones among women and men. *Kidney Int.* **2001**, *59*, 2290–2298.
- (10) Weber, S.; Schneider, L.; Peters, M.; Misselwitz, J.; Ronnefarth, G.; Boswald, M.; Bonzel, K. E.; Seeman, T.; Sulakova, T.; Kuwertz-Broking, E.; Gregoric, A.; Palcoux, J. B.; Tasic, V.; Manz, F.; Scharer, K.; Seyberth, H. W.; Konrad, M. Novel paracellin-1 mutations in 25 families with familial hypomagnesemia with hypercalciuria and nephrocalcinosis. *J. Am. Soc. Nephrol.* **2001**, *12*, 1872–1881.
- (11) Ludwig, M.; Utsch, B.; Balluch, B.; Frund, S.; Kuwertz-Broking, E.; Bokenkamp, A. Hypercalciuria in patients with CLCN5 mutations. *Pediatr. Nephrol.* **2006**, *21*, 1241–1250.
- (12) Stapleton, F. B.; Miller, L. A. Renal function in children with idiopathic hypercalciuria. *Pediatr. Nephrol.* **1988**, *2*, 229–235.
- (13) Bonilla-Felix, M.; Villegas-Medina, O.; Vehaskari, V. M. Renal acidification in children with idiopathic hypercalciuria. *J. Pediatr.* **1994**, 124, 529–534.
- (14) Worcester, E. M.; Gillen, D. L.; Evan, A. P.; Parks, J. H.; Wright, K.; Trumbore, L.; Nakagawa, Y.; Coe, F. L. Evidence that postprandial reduction of renal calcium reabsorption mediates hypercalciuria of patients with calcium nephrolithiasis. *Am. J. Physiol Renal Physiol.* **2007**, 292, F66–F75.
- (15) Akil, I.; Kavukcu, S.; Inan, S.; Yilmaz, O.; Atilla, P.; Islekel, H.; Nese, N.; Muftuoglu, S. Evaluation of histologic changes in the urinary tract of hypercalciuric rats. *Pediatr. Nephrol.* **2006**, *21*, 1681–1689.
- (16) Unwin, R. J.; Capasso, G.; Shirley, D. G. An overview of divalent cation and citrate handling by the kidney. *Nephron Physiol.* **2004**, 98, 15–20.
- (17) Boros, S.; Bindels, R. J.; Hoenderop, J. G. Active Ca(2+) reabsorption in the connecting tubule. *Pfluegers Arch.* **2009**, 458, 99–109
- (18) Lieske, J. C.; Deganello, S. Nucleation, adhesion, and internalization of calcium-containing urinary crystals by renal cells. *J Am. Soc. Nephrol.* **1999**, *10* (Suppl14), S422–S429.
- (19) Rindler, M. J.; Chuman, L. M.; Shaffer, L.; Saier, M. H., Jr. Retention of differentiated properties in an established dog kidney epithelial cell line (MDCK). *J. Cell Biol.* 1979, 81, 635–648.
- (20) Saier, M. H., Jr. Growth and differentiated properties of a kidney epithelial cell line (MDCK). *Am. J. Physiol.* **1981**, 240, C106–C109.
- (21) Jensen, L. J.; Kuhn, M.; Stark, M.; Chaffron, S.; Creevey, C.; Muller, J.; Doerks, T.; Julien, P.; Roth, A.; Simonovic, M.; Bork, P.; von Mering, C. STRING 8--a global view on proteins and their functional interactions in 630 organisms. *Nucleic Acids Res.* **2009**, *37*, D412–D416.

- (22) Fong-ngern, K.; Chiangjong, W.; Thongboonkerd, V. Peeling as a novel, simple, and effective method for isolation of apical membrane from intact polarized epithelial cells. *Anal. Biochem.* **2009**, *395*, 25–32.
- (23) Thongboonkerd, V.; Semangoen, T.; Chutipongtanate, S. Factors determining types and morphologies of calcium oxalate crystals: Molar concentrations, buffering, pH, stirring and temperature. *Clin. Chim. Acta* **2006**, *367*, 120–131.
- (24) Rodriguez, L. G.; Wu, X.; Guan, J. L. Wound-healing assay. *Methods Mol. Biol.* **2005**, 294, 23–29.
- (25) Storesund, T.; Hayashi, K.; Kolltveit, K. M.; Bryne, M.; Schenck, K. Salivary trefoil factor 3 enhances migration of oral keratinocytes. *Eur. J. Oral Sci.* **2008**, *116*, 135–140.
- (26) Megevand, M.; Favre, H. Distal renal tubular dysfunction: a common feature in calcium stone formers. *Eur. J. Clin. Invest.* **1984**, *14*, 456–461.
- (27) Lim, L. H.; Pervaiz, S. Annexin 1: the new face of an old molecule. *FASEB J.* **2007**, *21*, 968–975.
- (28) Wang, L. P.; Bi, J.; Yao, C.; Xu, X. D.; Li, X. X.; Wang, S. M.; Li, Z. L.; Zhang, D. Y.; Wang, M.; Chang, G. Q. Annexin A1 expression and its prognostic significance in human breast cancer. *Neoplasma* **2010**, *57*, 253–259.
- (29) Yu, G.; Wang, J.; Chen, Y.; Wang, X.; Pan, J.; Li, Q.; Xie, K. Tissue microarray analysis reveals strong clinical evidence for a close association between loss of annexin A1 expression and nodal metastasis in gastric cancer. *Clin. Exp. Metastasis* **2008**, *25*, 695–702.
- (30) Wang, K. L.; Wu, T. T.; Resetkova, E.; Wang, H.; Correa, A. M.; Hofstetter, W. L.; Swisher, S. G.; Ajani, J. A.; Rashid, A.; Hamilton, S. R.; Albarracin, C. T. Expression of annexin A1 in esophageal and esophagogastric junction adenocarcinomas: association with poor outcome. *Clin. Cancer Res.* **2006**, *12*, 4598–4604.
- (31) Perretti, M.; Dalli, J. Exploiting the Annexin A1 pathway for the development of novel anti-inflammatory therapeutics. *Br. J. Pharmacol.* **2009**, *158*, 936–946.
- (32) McArthur, S.; Cristante, E.; Paterno, M.; Christian, H.; Roncaroli, F.; Gillies, G. E.; Solito, E. Annexin A1: a central player in the anti-inflammatory and neuroprotective role of microglia. *J. Immunol.* **2010**, *185*, 6317–6328.
- (33) John, C. D.; Gavins, F. N.; Buss, N. A.; Cover, P. O.; Buckingham, J. C. Annexin A1 and the formyl peptide receptor family: neuro-endocrine and metabolic aspects. *Curr. Opin. Pharmacol.* **2008**, 8, 765–776
- (34) Pieretti, S.; Di Giannuario, A.; De Felice, M.; Perretti, M.; Cirino, G. Stimulus-dependent specificity for annexin 1 inhibition of the inflammatory nociceptive response: the involvement of the receptor for formylated peptides. *Pain* **2004**, *109*, 52–63.
- (35) Thurgood, L. A.; Wang, T.; Chataway, T. K.; Ryall, R. L. Comparison of the specific incorporation of intracrystalline proteins into urinary calcium oxalate monohydrate and dihydrate crystals. *J. Proteome. Res.* **2010**, *9*, 4745–4757.
- (36) Alldridge, L. C.; Bryant, C. E. Annexin 1 regulates cell proliferation by disruption of cell morphology and inhibition of cyclin D1 expression through sustained activation of the ERK1/2 MAPK signal. *Exp. Cell Res.* **2003**, 290, 93–107.
- (37) Croxtall, J. D.; Choudhury, Q.; Flower, R. J. Inhibitory effect of peptides derived from the N-terminus of lipocortin 1 on arachidonic acid release and proliferation in the A549 cell line: identification of E-Q-E-Y-V as a crucial component. *Br. J. Pharmacol.* **1998**, *123*, *975*–*983*.
- (38) Xia, S. H.; Hu, L. P.; Hu, H.; Ying, W. T.; Xu, X.; Cai, Y.; Han, Y. L.; Chen, B. S.; Wei, F.; Qian, X. H.; Cai, Y. Y.; Shen, Y.; Wu, M.; Wang, M. R. Three isoforms of annexin I are preferentially expressed in normal esophageal epithelia but down-regulated in esophageal squamous cell carcinomas. *Oncogene* **2002**, *21*, 6641–6648.
- (39) Kang, J. S.; Calvo, B. F.; Maygarden, S. J.; Caskey, L. S.; Mohler, J. L.; Ornstein, D. K. Dysregulation of annexin I protein expression in high-grade prostatic intraepithelial neoplasia and prostate cancer. *Clin. Cancer Res.* **2002**, *8*, 117–123.
- (40) Xiao, G. S.; Jin, Y. S.; Lu, Q. Y.; Zhang, Z. F.; Belldegrun, A.; Figlin, R.; Pantuck, A.; Yen, Y.; Li, F.; Rao, J. Annexin-I as a potential target for

Journal of Proteome Research

- green tea extract induced actin remodeling. *Int. J. Cancer* **2007**, *120*, 111–120.
- (41) Perretti, M.; Croxtall, J. D.; Wheller, S. K.; Goulding, N. J.; Hannon, R.; Flower, R. J. Mobilizing lipocortin 1 in adherent human leukocytes downregulates their transmigration. *Nat. Med.* **1996**, *2*, 1259–1262.
- (42) Getting, S. J.; Flower, R. J.; Perretti, M. Inhibition of neutrophil and monocyte recruitment by endogenous and exogenous lipocortin 1. *Br. J. Pharmacol.* **1997**, *120*, 1075–1082.
- (43) Perretti, M.; Ingegnoli, F.; Wheller, S. K.; Blades, M. C.; Solito, E.; Pitzalis, C. Annexin I modulates monocyte-endothelial cell interaction in vitro and cell migration in vivo in the human SCID mouse transplantation model. *J. Immunol.* **2002**, *169*, 2085–2092.
- (44) Rescher, U.; Danielczyk, A.; Markoff, A.; Gerke, V. Functional activation of the formyl peptide receptor by a new endogenous ligand in human lung A549 cells. *J. Immunol.* **2002**, *169*, 1500–1504.
- (45) Im, M. J.; Hoopes, J. E. Enzyme activities in regenerating epithelium during wound healing. IV. Aminotransferases and NADP-dependent enzymes. *J. Surg. Res.* **1973**, *15*, 262–270.
- (46) Dunham, J.; Shedden, R. G.; Catterall, A.; Bitensky, L.; Chayen, J. Pentose-shunt oxidation in the periosteal cells in healing fractures. *Calcif. Tissue Res.* **1977**, 23, 77–81.
- (47) Buchholz, B.; Teschemacher, B.; Schley, G.; Schillers, H.; Eckardt, K. U. Formation of cysts by principal-like MDCK cells depends on the synergy of cAMP- and ATP-mediated fluid secretion. *J Mol. Med.* **2011**, 89, 251–261.
- (48) Dos Santos, P. M.; Freitas, F. P.; Mendes, J.; Tararthuch, A. L.; Fernandez, R. Differential regulation of H+-ATPases in MDCK-C11 cells by aldosterone and vasopressin. *Can. J. Physiol. Pharmacol.* **2009**, 87, 653–665.
- (49) Evan, A. P.; Lingeman, J. E.; Coe, F. L.; Parks, J. H.; Bledsoe, S. B.; Shao, Y.; Sommer, A. J.; Paterson, R. F.; Kuo, R. L.; Grynpas, M. Randall's plaque of patients with nephrolithiasis begins in basement membranes of thin loops of Henle. *J. Clin. Invest.* 2003, 111, 607–616.
- (50) Bushinsky, D. A. Nephrolithiasis: site of the initial solid phase. *J. Clin. Invest.* **2003**, *111*, 602–605.